ISSN 0869-5938, Stratigraphy and Geological Correlation, 2006, Vol. 14, No. 6, pp. 581–601. © MAIK "Nauka/Interperiodica" (Russia), 2006.
Original Russian Text © O.M. Rosen, L.K. Levskii, D.Z. Zhuravlev, A.Ya. Rotman, Z.V. Spetsius, A.F. Makeev, N.N. Zinchuk, A.V. Manakov, V.P. Serenko, 2006, published in Stratigrafiya. Geologicheskaya Korrelyatsiya, 2006, Vol. 14, No. 6, pp. 3–24.

# Paleoproterozoic Accretion in the Northeast Siberian Craton: Isotopic Dating of the Anabar Collision System

**O. M. Rosen[a], L. K. Levskii[b], D. Z. Zhuravlev[c], A. Ya. Rotman[e], Z. V. Spetsius[d], A. F. Makeev[b], N. N. Zinchuk[e], A. V. Manakov[e], and V. P. Serenko[e]**

[a] *Geological Institute, Russian Academy of Sciences, Pyzhevskii per. 7, Moscow, 119017 Russia*
*e-mail: roseno@ilran.ru*

[b] *Institute of Precambrian Geology and Geochronology, Russian Academy of Sciences, nab. Makarova 2, St. Petersburg, 199034 Russia*

[c] *Institute of Mineralogy and Geochemistry of Rare Elements, Ministry of Natural Resources, Moscow, Russia*

[d] *Yakutniipromalmaz, AK ALROSA, Mirnyi, Russia*

[e] *Yakut Research and Geological Prospecting Enterprise, AK ALROSA, Mirnyi, Russia*

Received August 2, 2005; in final form, February 10, 2006

**Abstract**—Geochronological database considered in the work and characterizing the Anabar collision system in the Northeast Siberian craton includes coordinated results of Sm–Nd and Rb–Sr dating of samples from crustal xenoliths in kimberlites, deep drill holes, and bedrock outcrops. As is inferred, collision developed in three stages dated at 2200–2100, 1940–1760, and 1710–1630 Ma. The age of 2000–1960 Ma is established for substratum of mafic rocks, which probably originated during the lower crust interaction with asthenosphere due to the local collapse of the collision prism. Comparison of Sm–Nd and Rb–Sr isochron dates shows that the system cooling from ≈700 to ≈300°C lasted approximately 300 m.y. with a substantial lag relative to collision metamorphism and granite formation. It is assumed that accretion of the Siberian craton resulted in formation of a giant collision mountainous structure of the Himalayan type that was eroded by 1.65 Ga ago, when accumulation of gently dipping Meso- to Neoproterozoic (Riphean) platform cover commenced.

**DOI:** 10.1134/S0869593806060013

*Key words*: Sm–Nd and Rb–Sr isotopic dating, Early Precambrian, Earth crust, accretion, collision, kimberlite, diamond, Siberian craton.

## INTRODUCTION

The isotopic–geochronological study of Early Precambrian collision systems is usually limited by dating granitoids, and the dates obtained are interpreted as characterizing age of continental collision. In fact, this is not quite correct. Granitoid magmatism postdates collision of crustal blocks by 25 m.y. and its long pulses are separated by periods that lasted tens million years. The collision prism cooling is similarly a long process. The purpose of this study is to determine geochronology of metamorphism and cooling of the Paleoproterozoic Anabar collision system and to elucidate the Siberian craton evolution and some peculiarities in development of that system, i.e., the local collapse and relevant specific magmatism, which are characteristic of Phanerozoic collision systems. The Yakut diamond-bearing province situated in the study region determines an elevated interest to the region structure and evolution. Stratigraphic and chronological terminology is consistent with that accepted in recent works (Semikhatov, 1993; Akhmedov et al., 2001; Gradstein et al., 2004).

## SIBERIAN CRATON AND ANABAR COLLISION SYSTEM

The Siberian craton approximately $4 \times 10^6$ km$^2$ in size is largely (70%) overlain by Riphean–Phanerozoic sedimentary cover 1–8 km thick. It is bordered by the Taimyr and Verkhoyansk foldbelts of the Phanerozoic foreland in the north and east and by the Paleozoic Central Asian and Mesozoic Mongol–Okhotsk volcanic orogenic belts in the west and south. The Anabar collision system occupies approximately one third of the Siberian craton and extends for 1500 and 600–900 km in meridional and latitudinal directions, respectively. The consolidated crust beneath the system is thicker (58 km according to Manakov, 1999) than the averaged crustal thickness of ~ 40 km estimated for old cratons. The thickness anomaly is usually interpreted as corresponding to relict of an old collision prism (Parfenuk and Mareschal, 1997; Parfenuk, 2004). Considered below are isotopic-geochronological data known prior to this study.

Terranes and sutures (collision zones) are principal units regarded by historical–geological analysis. The

isotopic dates have been used to elaborate the historical–geological models of the craton evolution (Rosen et al., 1994, 2000; Popov and Smelov, 1996; Frost et al., 1998; and others). The present-day structure of craton is generally considered as a result of collision, amalgamation and accretion of microcontinents different in age, which turned into heterogeneous tectonic blocks (terranes) in the course of collision (Rosen et al., 1994, 2003; Smelov et al., 1998a) that is consistent with the current concept of accretionary tectonics (Sokolov, 2003). As was shown, these events took place ~1.8–1.9 Ga ago concurrently to amalgamation of other cratons, and the Siberian craton was assumed to be a part of the supercontinent Pangea-1 (Rosen, 2002). Faults separating terranes reveal structural features of tectonic compression and thrusting, which are characteristic of sutures or collision zones. It is established that local metamorphism and granite formation in sutures were concurrent to granulite metamorphism in neighboring terranes. This synchronism could be caused only by spontaneous heating (thermal relaxation) inside the thickened crust of the collision prism, as it is evident from theoretical models (England and Thompson, 1984; Le Pichon et al., 1997) and geological observations (Rosen and Fedorovskii, 2001; Diaconescu and Knapp, 2002). Granitoid magmatism takes place only 25 m.y. after immediate collision of blocks, and long pulses of this magmatic activity can be separated by periods tens million years long. Cooling of the collision prism is similarly a long process (England and Thompson, 1984; Nironen et al., 2000).

Granulite-gneiss and granite-greenstone areas distinguished long ago in the Siberian craton (Petrov et al., 1985) correspond to relevant terranes, which are of different age according to recent data. The terranes are composed of variable rock associations and reveal individual character of magnetic and gravity fields (Rosen, 2003). The granulite–gneiss associations are presumably of volcanogenic island-arc origin (Rosen, 1992), being composed in general of orthopyroxene plagiogneisses and mafic metamorphites deformed into isoclinal folds and characterized by linear magnetic and gravity anomalies. They represent lower crustal rocks. Dominant in granite–greenstone associations of the upper crust are amoeboid bodies of granitoids (80–90%) with intervening synforms composed of mafic volcanic and intrusive rocks associated with subordinate graywackes. Although both associations can theoretically be seen as juxtaposed on the erosion surface of the terrane, the accepted binary discrimination of terranes is consistent with recent observations and represents necessary working simplification and useful investigation tool.

**The Siberian craton structure.** Prior to their amalgamating into a common craton, terranes grouped into tectonic provinces (superterranes, composite terranes in terminology of Sokolov, 2003). Their collision and amalgamation resulted in the formation of the Siberian craton. The craton comprises the Tungus, Anabar, Olenek, Aldan, and Stanovoi provinces (Fig. 1). The latter consist of heterogeneous terranes (tectonic blocks) with superimposed Early Proterozoic fold and orogenic belts sometimes. Areas between terranes correspond to Paleoproterozoic island-arc fragments (Smelov et al., 2002), the largest among which is the Akitkan orogenic belt. The belt represents a Paleoproterozoic island-arc system sandwiched between the Anabar and Aldan superterranes. The system development terminated by the collision prism collapse 1.8 Ga ago. This event was accompanied by emplacement of A-granites of specific geochemical type (Neimark et al., 1998). The central and northeastern parts of the craton are occupied by the Anabar collision system that comprises the Anabar and Olenek tectonic provinces.

**The Anabar province** includes the Magan and Daldyn granulite–gneiss terranes exposed in the Anabar shield and composed of rocks dated at 2.9 and 3.1 Ga, respectively. Granulite metamorphism and granitoid magmatism are estimated to be 1.8 and 1.9 Ga old. The Anabar province includes also the Markha granite–greenstone terrane in the eponymous river basin, where it is overlain by sedimentary cover being studied via boreholes. Substratum and metamorphism of the last terrane are dated at 2.5 and 1.76 Ga, respectively (Neimark et al., 1992; Rosen at al., 2002).

The *Kotuikan suture* (collision zone) between the Daldyn and Magan terranes (Fig. 2) is a few to 30 km wide, being represented by tectonic blastomylonitic macromelange. The apomylonite matrix turned into gneissic migmatite (amphibolite metamorphic facies) encloses concordant to discordant vein-shaped bodies of autochthonous granites 1.8–2.0 Ga old, tectonic blocks of anorthosites and large, up to tens kilometers long, granulite blocks detached from adjacent terranes and subjected to retrograde amphibolite metamorphism

**Fig. 1.** Geological structure of the study area. (A) Position of the Siberian craton in the northeastern Eurasia. (B) Main tectonic elements of the Siberian craton: (1) Archean terranes, 3.5–2.5 Ga, granite–greenstone (a) and granulite–gneiss (b); (2) Proterozoic fold belts, 2.4–2.0 Ga; (3) exposed areas of the basement; (4) fault zone bordering the craton (a) and sutures in the craton limits (b). (C) Structure of the Anabar collision system and its flanks (Rosen, 2003): (1) main fault zones (collision zones, sutures); (2) other faults; (3) contours of exposed areas; (4) platform cover, the thickness exceeds 8 km; (5) kimberlite fields Muna (*1*), Daldyn (*2*), Alakit (*3*) and Mirnyi (*4*) with dated crustal xenoliths; (6) gabbro–anorthosite complex, 2.55 Ga; (7) calc-alkaline volcanics, sediments, A-granite; (8) felsic volcanics, siliciliths, granites, 1.85 Ga (a), paragneisses and metacarbonates, 2.4–2.0 Ga (b); (9) granite–greenstone complex: (gs) greenstone belts and mafic intrusions (Gafarov et al., 1978), (gr) large granitoid intrusions (*The Map of Metamorphic…*, 1987), 2.5–2.9 Ga; (10) complex of plagiogranites, enderbites, and mafic granulites, 3.1–3.0 Ga. Terranes: Markha, Birekte (granite–greenstone), Magan, Daldyn (granulite–gneiss).

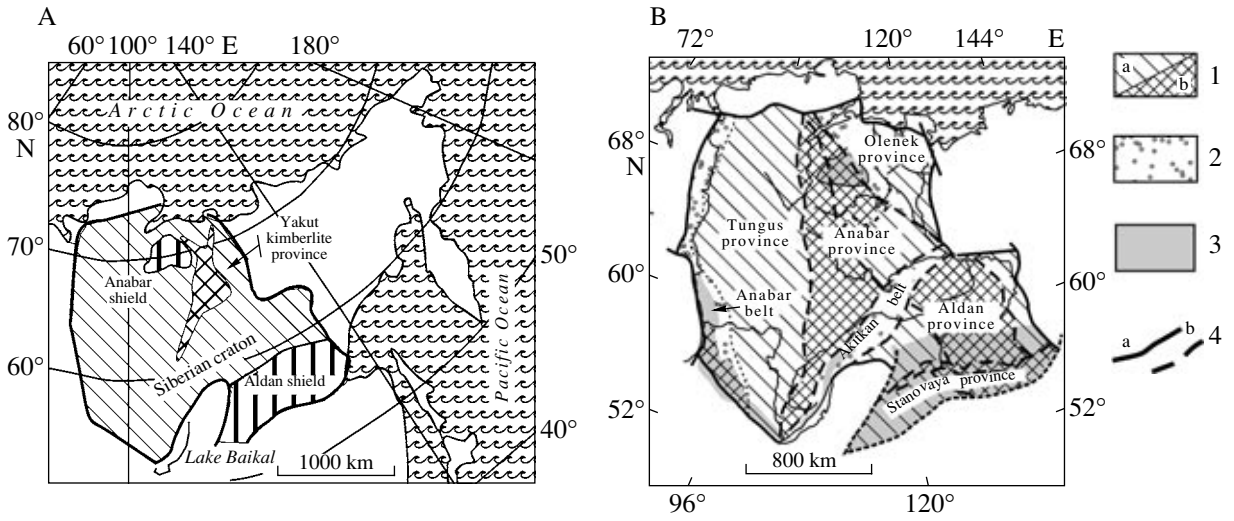
A
60° 100° 140° E 180°
80° N
70°
60°
50°
40°
Arctic Ocean
Pacific Ocean
Yakut kimberlite province
Anabar shield
Siberian craton
Aldan shield
Lake Baikal
1000 km
B
72° 120° 144° E
68° N
60°
52°
96° 120°
Olenek province
Tungus province
Anabar province
Anabar belt
Aldan province
Akitkan belt
Stanovaya province
800 km
a b 1
2
3
a b 4

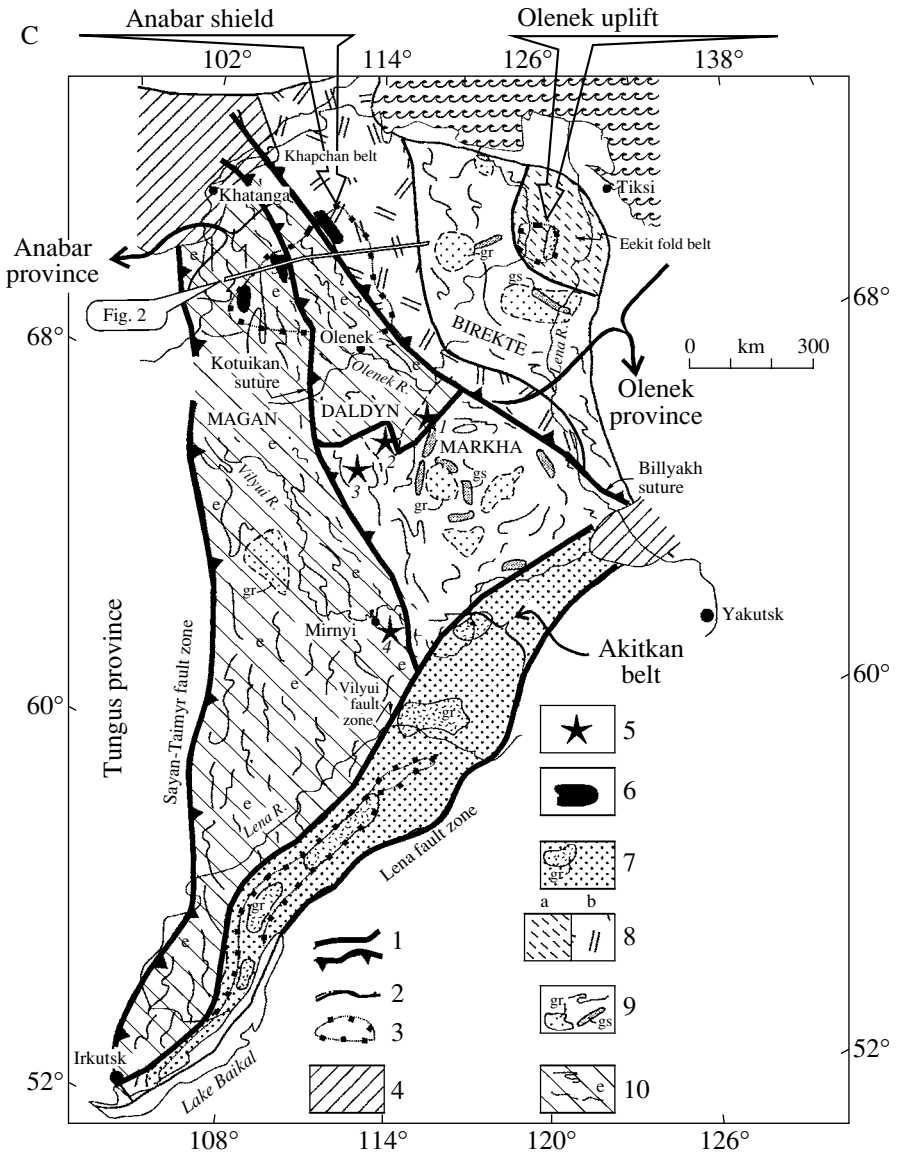
C
Anabar shield
Olenek uplift
102° 114° 126° 138°
68°
60°
52°
108° 114° 120° 126°
Khapchan belt
Khatanga
Tiksi
Eekit fold belt
Anabar province
Fig. 2
Olenek
Olenek R.
Kotuikan suture
BIREKTE
Lena R.
0 km 300
Olenek province
MAGAN
DALDYN
MARKHA
Billyakh suture
Vilyui R.
Yakutsk
Mirnyi
Akitkan belt
Tungus province
Sayan-Taimyr fault zone
Vilyui fault zone
Lena fault zone
Lena R.
Irkutsk
Lake Baikal
1
2
3
4
5
6
7
a b 8
9
10

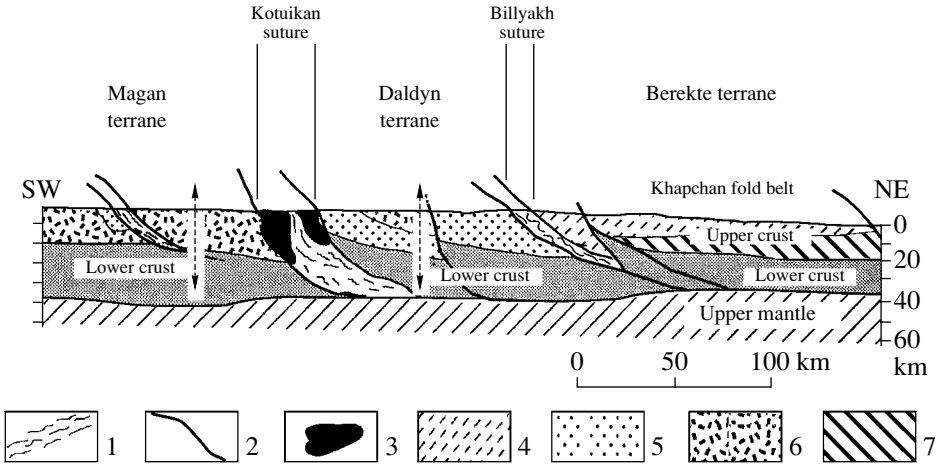


**Fig. 2.** Schematic cross section of the Anabar collision system (Rosen et al., 1994; Rosen, 2003): (1) main fault zones (sutures): tectonic melangé with apomylonite magmatite matrix, 1.9–1.8 Ga; (2) thrust surface; (3) anorthosite and gabbro, 2.55 Ga; (4) granulite metagraywacke and metacarbonate, 2.4–2.0 Ga; (5) plagiogneiss, enderbite, and mafic granulite 3.1–3.0 Ga; (6) plagiogneiss, enderbite, charnockite, 3.0–2.9 Ga; (7) granite–greenstone association, 2.5 Ga. Position of the lower and upper crust is shown for the visual assessment of the erosion depth in the collision system.

(Rachkov, 1988; Lutts and Oksman, 1990). Characteristic of the melangé are fragments of island-arc volcanics (Smelov et al., 2002) and lenticular interbeds of sedimentary quartzites, carbonates, and metavolcanic high-magnesian amphibolites concordant with tectonic foliation and probably representing disconnected fragments of deposits, which accumulated in intercontinental basins and were involved into collision. This was a substance of lowered viscosity (accretionary wedge in terminology of Dobretsov et al., 2001) in frontal parts of collided microcontinents and fragments of island-arc volcanics (Smelov et al., 2002).

The *Billyakh suture* separates the Anabar and Olenek provinces. Granulites of the Khapchan belt confined to this suture were metamorphosed 1.97 Ga ago. Collision migmatites and granitoids are dated at 1.8 Ga (Rosen et al., 2000).

*Older collision processes* took place probably at the boundary between the Markha (substance 2.5 Ga old) and Daldyn (3.1 Ga) terranes. Age of the collision suture can approximately be estimated as 2.2–2.3 Ga, i.e., older than the Billyakh and Kotuikan sutures truncating it in the east, as is evident from geological relationships. In addition, there are known relicts of Archean granulite metamorphism (2.76 Ga ago) within the Daldyn terrane (Rosen et al., 2000). Taking into consideration the age relationship between granulite metamorphism in terranes, on the one hand, and granite formation and metamorphism in neighboring collision zones, on the other, we can suggest the age value of 2.76 Ga for the oldest collision event in the region, although spatial configuration of collided objects is unknown so far. Rosen (2003) arrived at the conclusion that there were three collision epochs: younger in the terminal Paleoproterozoic, intermediate approximately 2.2 to 2.1 Ga ago (middle Paleoproterozoic), and older 2.8 Ga ago (Neoarchean). The Kotuikan and Billyakh sutures mark the central part of the Anabar collision system.

The **Olenek province** comprises heterogeneous tectonic elements. In the Anabar shield located in the western part of the province, there are hosts outcrops of granulite metagraywackes (garnet gneisses) and metacarbonates (calcareous–silicate rocks and calciphyres) of the *Khapchan fold belt.* Ages of clastic material and granulite metamorphism are 2.4 and 1.97 Ga, respectively (Rosen et al., 2000). Clastic material was likely derived from eroded basement of the Birekte granite–greenstone terrane (now entirely overlain by sedimentary cover), while sediments of the Khapchan belt accumulated presumably at its passive (western in present-day coordinates) margin. The Olenek uplift, where the eastern active margin of the terrane was located, accumulated acid volcanics and carbonaceous siliciliths of the *Eekit fold belt*, which experienced greenschist facies metamorphism 1.98 Ga ago and were intruded by granitoids approximately 1.85 Ga ago (Rosen et al., 2000).

*Previous isotopic–geochronological studies.* Rosen (2002) summarized almost all the previous age estimates obtained for consolidated crust of the Siberian craton (224 dates in total), which were published in numerous works (Neimark et al., 1992, 1998; Kovach, 1994; Rizvanova et al., 1994; Rozen et al., 1994, 2000; Frost et al., 1998; Jahn et al., 1998; Shemyakin et al., 1998; Kovach et al., 1999; Kotov et al., 1999; and others). These and later data (Larin et al., 2003, Levitskii et al., 2004; Sal'nikova et al., 2004; Turkina, 2004; Donskaya et al., 2005; and others) are presented in Fig. 3. The Sm–Nd model ages and U–Pb dates obtained for magmatic zircons suggest that juvenile matter was derived from depleted mantle ~ 3.3 and ~ 3.0 Ga ago in

granulite–gneiss terranes and ~ 3.5 and ~ 2.5 Ga ago in granite–greenstone terranes.

Zircon dates and model T(DM)Nd values of 2.2–2.4 Ga characterize fold belts. Their sedimentary and volcanogenic complexes accumulated on surface of microcontinents prior to accretion (sediments of the Khapchan belt in the Anabar shield, the Ungra mafites and greenstones of the Kholdnikan belt in the Aldan shield, and some others). Zircons from collision granites and charnockites are dated at 1.7–2.0 Ga. It is established that U–Pb zircon ages determined for migmatites and granites of the Anabar shield coincide with the granulite metamorphism age estimates based on Sm–Nd mineral isochrons (1.8–1.9 Ga). Synchronism of two thermal petrogenetic events is indispensable consequence of the thermal regime in thickened crust of the collision prism (self-heating). Juvenile material probably did not ascend from the mantle in the course of accretion, since Sm–Nd model ages younger than 2.1 Ga are unknown, and collision granitoids originated from sialic crust of old microcontinents. The lithospheric mantle activation by the collision prism collapse at that time is however evident from model ages of lamproites (T(DM)Nd = 2.1–2.2 Ga) that intruded 1.3 Ga ago the Urik–Iya fold belt of the Biryusa terrane in the Sayan region (Egorov et al., 2005).

## PECULIARITIES OF ROCK FORMATION IN COLLISION SYSTEMS

Evolution of a collision system consists of separate episodes (stages), which can be recurrent. The crust thickens first due to collision and thrusting of continental blocks above a circulating mantle cell. Coupling of heat flows puts in action the self-heating mechanism that increases temperature 25 m.y. later to the level sufficient for generation of granitic magmas synkinematic at least, localized in the lit-par-lit manner and accompanied by migmatization. The above time span is estimated based on the crust thermal conductivity, heat flow values, and other parameters (England and Thompson, 1984). It is consistent with data on Himalayas, where collision commenced 50 Ma ago, while leucogranites originated 25–28 Ma ago (Rosen and Fedorovskii, 2001). Compression can give way to tension, and two regimes may alternate during tens million years (Selverstone, 2005). When the crust reaches some critical thickness and its viscosity sharply drops under elevating temperature, this leads to the lower crust extension and collapse of the orogenic structure. The temporal (local) cessation of collision-related compression eliminates the thermal crust–mantle boundary and hot asthenosphere interacts with the crust (Searle, 1999). The interaction provokes melting in the lower crust without migmatization and gives rise to origin of postkinematic A-granite intrusions with specific geochemical characteristics and associated mafic rocks. This petrological scenario was explained in hypotheses of basalt underplating (Kay and Kay, 1993) and detachment of subducting slabs (Davies and von Blankenburg, 1995), which have no factual difference in terms of general petrology of collision orogens (Vladimirov et al., 2003).

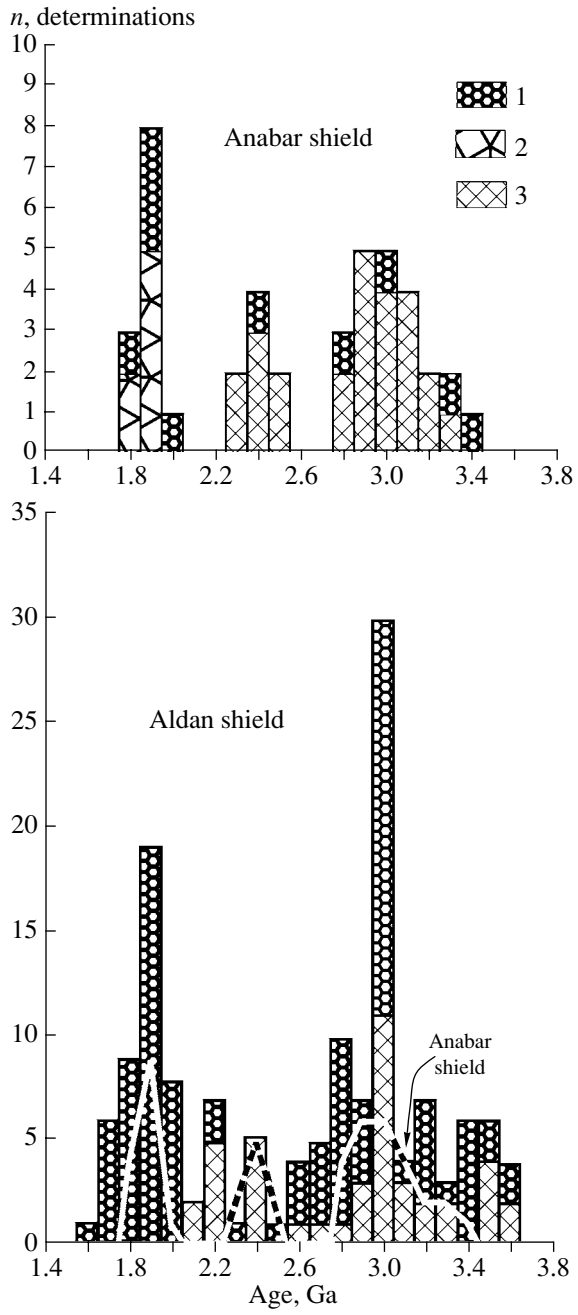


**Fig. 3.** Histograms demonstrating distribution of isotopic ages determined for main structures of the Siberian craton: (1) U–Pb method, zircon, upper intersection; (2, 3) Sm–Nd method: (2) mineral isochron, (3) model age, T(Nd)DM.

In the above consideration of the Siberian craton geochronological evolution, we stressed only main events in geologic history of the craton proper and its collision systems. Samples sporadicly collected from outcrops are insufficient, even being reliably dated, for

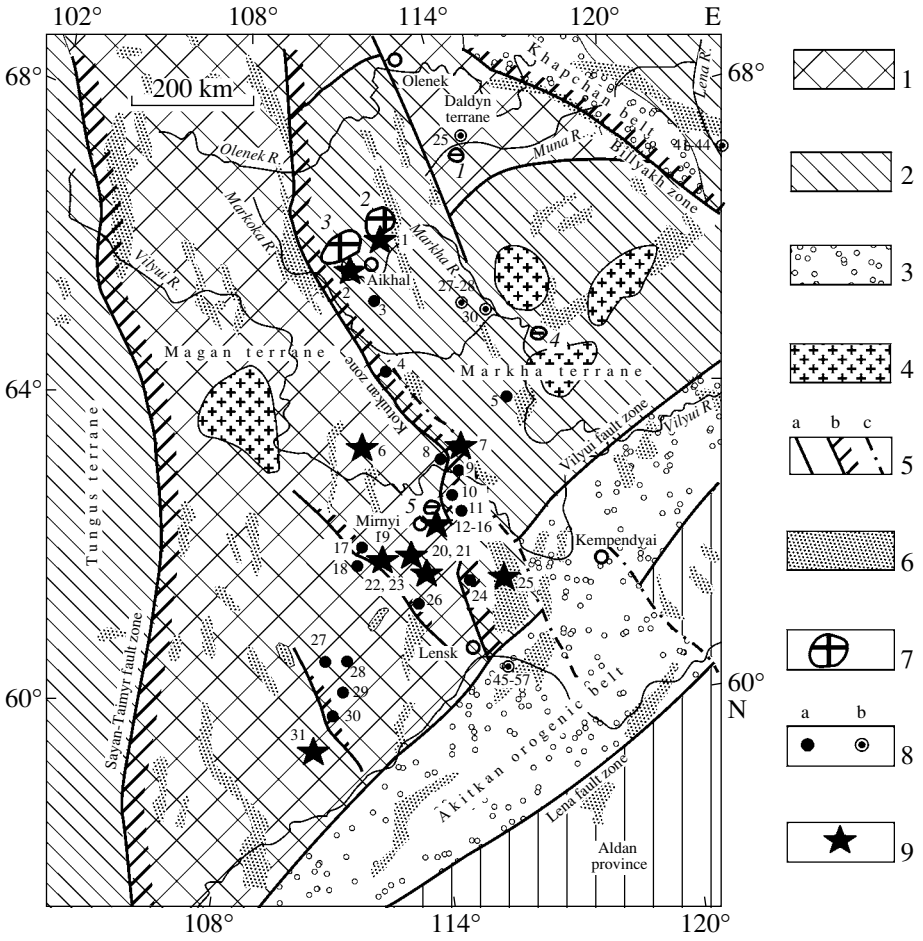


**Fig. 4.** Schematic geological structure of the basement and location of boreholes in the central part of the Anabar collision system (Rosen et al., 2002): (1) granulite–gneiss terrane; (2) granite–greenstone terrane; (3) metamorphosed volcanics, sediments, granitoid fold belts; (4) granite batholith (*The Map of Metamorphic…*, 1987); (5) Early Proterozoic suture (a), the same, thrusts with the NE dip (b), Phanerozoic sutures (strike slip faults) (c); (6) positive magnetic anomalies ΔTa exceeding +5 Me (Litvinova et al., 1978) and reflecting the basement structure; (7) kimberlite fields Muna (*1*), Daldyn (*2*), Alakit (*3*), Nakyn (*4*) and Mirnyi (*5*); (8a) boreholes and their numbers after Rosen et al. (2002), (8b) numbers of samples from boreholes (Smelov et al., 1998b); (9) boreholes with core samples studied in this work.

the comprehensive analysis of all events. Extrapolation of limited geochronological dates to spacious objects provokes tendency to date collision events with accuracy of few million years based on ages of crustal granitoids (e.g., Didenko et al., 2003; Donskaya et al., 2005; and references therein) that is not always correct.

The systematic dating of concrete objects shows that formation of collision granites is a process consisting of several pulses and lasting 50 to 100 m.y. For example, synkinematic microcline granitoids and migmatites related to collision in southern Finland were intruded 25 m.y. later by postkinematic granitoids (A-granites) accompanied by gabbroids in response to the collision prism collapse. The further development of accretion resulted in amalgamation of an additional continental mass and in origin of subsequent synkinematic granites and migmatites 40 m.y. later. The entire process lasted approximately 65 to 80 m.y. since 1.91–1.89 Ga until 1.84–1.83 Ga (Nironen et al., 2000).

## ISOTOPIC GEOCHRONOLOGY OF THE ANABAR COLLISION SYSTEM

**Materials.** The initial substratum, granulite metamorphism, and subsequent cooling events were dated by the Sm–Nd and Rb–Sr mineral isochron and whole-rock methods. Data on crustal xenoliths from kimberlites and drill-core samples from the depth interval of 2–4 km obtained in the Anabar collision system (Fig. 4) and published dates for sampled outcrops in the Anabar shield were also used in interpretations. Accordingly, it was possible to consider rock-forming processes based on samples from bedrock outcrops and different levels of the crust concealed under the platform cover, and to characterize thus the entire collision prism. The examined samples represent metamorphic rocks (except those from dolerite dike) that are classed with quartz-bearing gneisses and quartz-free crystalline schists or amphibolites (*Classification and Nomenclature…*, 1992).

Eclogite-like rocks are characterized by the elevated content of garnet. Characteristic minerals of the rocks are indicated in tables by symbols in the order of their content increase. Samples from *outcrops* of the Daldyn and Birekte terranes (Khapchan fold belt) of the Anabar shield are represented by granulites. *Drill-core sections* are largely composed of gneisses metamorphosed under conditions of amphibolite facies in the Markha terrane and of diaphtorites after granulites in the Magan terrane. Biotite granites intact and cataclastic have been examined as well. Petrography and chemical composition of these samples from boreholes have been described earlier (Rosen et al., 2002). *Crustal xenoliths from kimberlites* are dominated by crystalline schists corresponding in composition ($SiO_2$ = 49–52 wt %; $Al_2O_3$ = 14–22 wt %; MgO = 4–12 wt %; $Na_2O \geq K_2O$, up to 5.5 wt % in sum), like the eclogites-like rocks, to metabasalts. Cordierite-bearing rocks probably represent metapelites. Dolerite sample from a dike a few meters thick, crosscutting anorthosites of the Kotuikan suture shows no signs of metamorphic alteration (Rosen et al., 2000). Sampled rocks and their monomineral fractions are insignificantly affected by secondary alteration or unaltered.

**Methods.** The Sm, Nd, Rb, and Sr concentrations and isotopic composition were analyzed by the isotopic dilution method at the Institute of Precambrian Geology and Geochronology RAS (St. Petersburg) on the solid-phase 8-collector mass-spectrometer Finnigan MAT-261 in regime of simultaneous registration of ion currents. The analytical accuracy is ±0.3% (2σ) for $^{147}Sm/^{144}Nd$ ratios, ±0.5% (2σ) for $^{87}Rb/^{86}Sr$ ratios, and ±0.5% (2σ) for element concentrations. During measurements, isotopic parameters obtained for standard samples were as follows: La Jolla $^{143}Nd/^{144}Nd$ = 0.511879 ± 14 ($n$ = 45); $^{143}Nd/^{144}Nd$ BCR = 0.512673 ± 15 ($n$ = 10); $^{87}Sr/^{86}Sr$ BCR-1 = 0.705037 ± 50 ($n$ = 4); $^{87}Sr/^{86}Sr$ SRM-987 = 0.710249 ± 18. Blanks for Nd, Rb, and Sr were 0.5, 0.3, and 0.6 ng, respectively. The model age values are calculated based on the linear model of depleted mantle with parameters $^{147}Sm/^{144}Nd$ = 0.2136 and $^{143}Nd/^{144}Nd$ (0) = 513149.

**Results obtained by the Sm–Nd method and their interpretation.** Original and previously published analytical results (samples 6, 7, 16, 19–24 from Neimark et al., 1992, 25–27 from Bogatikov et al., 2004, and 31–35 from Rosen et al., 2000) are presented in Table 1. Age of metamorphism is determined based on mineral isochrons (Table 2). Because of contamination by kimberlite material or allochemical metamorphism, which influenced differently some minerals, the Sm–Nd method yields sometimes unsatisfactory results. In such a situation, we preferred based on two-point isochrons for a mineral and whole-rock data. This approach seems appropriate for getting the generalized parameters of rocks, although the latter sometimes experienced contamination by kimberlite melt. The pair of whole rock and garnet was most frequently used. In this case, the isochron characterizes age of specific

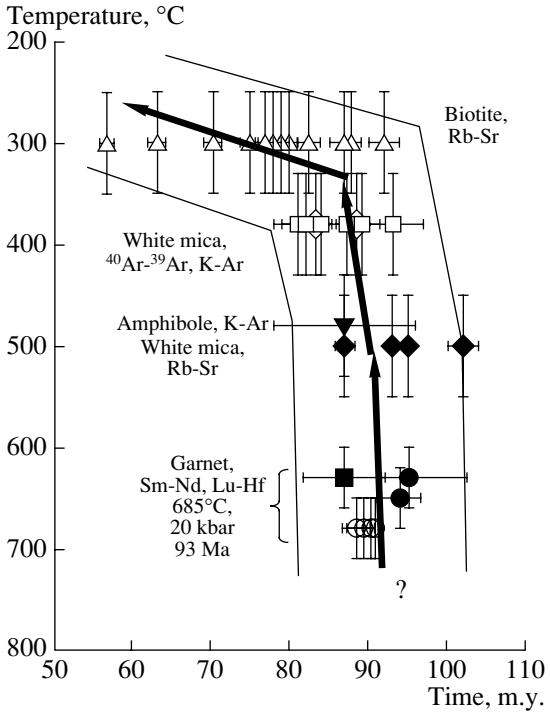


**Fig. 5.** Time–temperature relation for equilibration of isotope systems in minerals of the Eastern Alps collision system (Thöni, 2003).

metamorphic event (garnet growth) in distinction from the "average" age of metamorphism determined by polymineral isochrons plotted for minerals, which grew and became isotopically closed at different metamorphism stages (Baxter et al., 2002; Thöni, 2003). In the course of metamorphism, isotopic equilibration lasted for different minerals approximately 30 m.y. (Fig. 5). Garnets form at the peak of metamorphism antedating amphibole and magnesian micas by 7–9 and 20 m.y., respectively. Presence of mineral inclusions in garnet, e.g., of apatite, monazite, orthite, xenotime, and zircon, can distort age estimates (Prince et al., 2000; Thöni, 2003). Therefore, monomineral fractions were separated very carefully.

The Sm–Nd isochrons (whole rock–minerals) obtained for representative analyses of crustal xenoliths from kimberlites (Fig. 6) demonstrate that all the terranes yield three groups of dates approximating 1.65, 1.75, and 1.85 Ga that correspond probably to thermal events caused likely by paroxysms of terranes thrusting. Most intense distortions (Mirnyi and Daldyn fields) are probably caused by kimberlite melt penetration along cleavage and microfissures, which have not been detected during fraction examination under microscope. For example, Fig. 6e shows that the bulk eclogite-like rock is contaminated, and its age is determined therefore using minerals, which likely avoided contamination. Fig. 6l demonstrates that both the whole-rock sample of amphibolite and its minerals are contaminated. In this case, the estimated age character-

**Table 1.** Results of the Sm–Nd isotope analysis of samples from crustal xenoliths in kimberlites, drill cores, and outcrops

| No. | Sample number, analytical (original), rock | Material | Sm, μg/g | Nd, μg/g | $^{147}Sm/^{144}Nd$ | $^{143}Nd/^{144}Nd$ | $T^{DM}$, Ma | $T^{DM}$ 2st, Ma | εNd (T2) | εNd (T1) |
|---|---|---|---|---|---|---|---|---|---|---|
| 1 | 2 | 3 | 4 | 5 | 6 | 7 | 8 | 9 | 10 | 11 |
| 1 | 8-VK4, Pl-Grt-SCH | WR | 1.057 | 5.188 | 0.1232 | 0.511410 ± 12 | 2917 | 2903 | –7.4 | –0.3 |
| | | Grt | 0.984 | 2.620 | 0.2269 | 0.512612 ± 22 | | | | |
| | | Pl | 0.742 | 5.208 | 0.0862 | 0.510985 ± 25 | | | | |
| 2 | 12-VK4, Amp-Pl-Grt-SCH | WR | 1.087 | 4.143 | 0.1587 | 0.511807 ± 3 | 3698 | 3204 | –0.3 | –4.0 |
| | | Grt | 1.886 | 1.652 | 0.6906 | 0.518214 ± 25 | | | | |
| | | Pl | 0.129 | 1.349 | 0.0576 | 0.510590 ± 14 | | | | |
| | | Amp | 1.129 | 5.393 | 0.1265 | 0.511470 ± 19 | | | | |
| 3 | 13-VK4, Bt-Cpx-Pl-Grt-SCH | WR | 2.111 | 7.771 | 0.1642 | 0.512037 ± 3 | 3410 | 2980 | –4.0 | –1.3 |
| | | Grt | 1.757 | 1.362 | 0.7798 | 0.519470 ± 18 | | | | |
| | | Pl | 0.554 | 3.740 | 0.0895 | 0.511139 ± 12 | | | | |
| | | Cpx | 2.024 | 8.755 | 0.1398 | 0.512292 ± 18 | | | | |
| | | Bt | 0.480 | 2.160 | 0.1342 | 0.511909 ± 25 | | | | |
| 4 | 14-VK4, Bt-Pl-Grt-SCH | WR | 2.100 | 10.50 | 0.1209 | 0.511409 ± 8 | 2847 | 2843 | –6.7 | 0.4 |
| | | Grt | 3.231 | 3.695 | 0.5291 | 0.516176 ± 6 | | | | |
| | | Pl | 4.984 | 29.84 | 0.1009 | 0.511275 ± 20 | | | | |
| | | Bt | 1.274 | 7.738 | 0.0995 | 0.511110 ± 15 | | | | |
| 5 | 1-K11 (U-2295), Grt-Cpx-Pl-ECR | WR | 1.420 | 8.107 | 0.1059 | 0.511305 ± 10 | 2600 | 2613 | –6.6 | 3.2 |
| | | Grt | 1.144 | 2.031 | 0.3405 | 0.513393 ± 17 | | | | |
| | | Pl | 0.333 | 6.495 | 0.0309 | 0.510079 ± 5 | | | | |
| | | Cpx | 2.340 | 24.28 | 0.0583 | 0.510302 ± 5 | | | | |
| 6 | (U-2030a), Grt-Hb-Cpx-Opx-Pl-ECR | WR | 3.21 | 12.2 | 0.1588 | 0.512234* | 2537 | 2522 | 0.7 | 4.3 |
| | | Grt | 3.04 | 3.15 | 0.5850 | 0.517137* | | | | |
| | | Cpx | 4.27 | 16.0 | 0.1610 | 0.512214* | | | | |
| | | Pl | 0.212 | 2.02 | 0.0634 | 0.511171* | | | | |
| 7 | (U-2295-1), Ky-Grt-Cpx-Pl-ECR | WR | 1.311 | 7.76 | 0.1021 | 0.511322* | 2488 | 2486 | | 4.8 |
| 8 | 2-K11 (D-40), Grt-Cpx-Phl-SCH | WR | 10.95 | 59.84 | 0.1106 | 0.511322 ± 9 | 2691 | 2711 | –6.8 | 2.0 |
| | | Grt | 5.650 | 9.806 | 0.3482 | 0.513993 ± 11 | | | | |
| | | Cpx | 15.78 | 70.25 | 0.1358 | 0.511580 ± 11 | | | | |
| | | Phl | 2.105 | 13.92 | 0.0914 | 0.511165 ± 19 | | | | |
| | | Ap | 228.1 | 1188 | 0.1160 | 0.511319 ± 10 | | | | |
| 9 | 7-K11 (Zr-14), Grt-Pl-ECR | WR | 8.899 | 35.95 | 0.1496 | 0.512005 ± 11 | 2714 | 2646 | –2.5 | 2.8 |
| | | Grt | 6.175 | 8.151 | 0.4583 | 0.515319 ± 17 | | | | |
| | | Pl | 1.713 | 10.45 | 0.0991 | 0.511483 ± 11 | | | | |
| 10 | 8-K11 (S-45), Phl-Grt-Pl-GNS | WR | 7.375 | 44.56 | 0.1000 | 0.511614 ± 7 | 2055 | 1960 | 0.9 | 11.2 |
| | | Grt | 14.81 | 29.92 | 0.2993 | 0.513821 ± 12 | | | | |
| | | Pl | 4.405 | 30.86 | 0.0863 | 0.511215 ± 8 | | | | |
| | | Phl | 9.276 | 57.89 | 0.0969 | 0.511375 ± 8 | | | | |
| 11 | 9-K11 (S-84), Grt-Pl-Phl-GNS | WR | 7.922 | 47.64 | 0.1005 | 0.511394 ± 7 | 2357 | 2327 | –1.3 | 6.7 |
| | | Grt | 11.21 | 29.22 | 0.2320 | 0.512995 ± 8 | | | | |
| | | Pl | 2.641 | 19.37 | 0.0824 | 0.511220 ± 10 | | | | |
| | | Phl | 6.677 | 45.88 | 0.0880 | 0.511223 ± 3 | | | | |

**Table 1.** (Contd.)

| 1 | 2 | 3 | 4 | 5 | 6 | 7 | 8 | 9 | 10 | 11 |
|---|---|---|---|---|---|---|---|---|---|---|
| 12 | 10-K11 (S-86), Grt-Pl-Phl-SCH | WR | 11.11 | 58.84 | 0.1142 | 0.511550 ± 8 | 2442 | 2440 | –1.7 | 5.3 |
| | | Grt | 14.44 | 50.02 | 0.1745 | 0.512289 ± 5 | | | | |
| | | Pl | 8.682 | 56.32 | 0.0932 | 0.511310 ± 9 | | | | |
| | | Phl | 11.43 | 67.30 | 0.1026 | 0.511389 ± 5 | | | | |
| 13 | 11-K11 (S-99/463), Grt-Pl-Amp-Phl-GNS | WR | 4.589 | 23.29 | 0.1191 | 0.511555 ± 11 | 2561 | 2561 | –2.5 | 3.9 |
| | | Grt | 9.846 | 22.93 | 0.2596 | 0.513281 ± 5 | | | | |
| | | Pl | 3.324 | 27.41 | 0.0733 | 0.510981 ± 6 | | | | |
| | | Phl | 5.619 | 33.77 | 0.1006 | 0.511295 ± 22 | | | | |
| | | Amp | 1.995 | 11.00 | 0.1095 | 0.511427 ± 9 | | | | |
| 14 | 3-K11 (M-2017), Cpx-Pl-Phl-SCH | WR | 5.743 | 35.23 | 0.0985 | 0.511164 ± 5 | 2617 | 2575 | 1.6 | 6.7 |
| | | Pl | 1.808 | 12.41 | 0.0881 | 0.511173 ± 6 | | | | |
| | | Cpx | 15.52 | 88.26 | 0.1063 | 0.511031 ± 8 | | | | |
| | | Phl | 5.335 | 44.88 | 0.0718 | 0.510767 ± 5 | | | | |
| | | Ap | 26.13 | 147.5 | 0.1071 | 0.511080 ± 6 | | | | |
| 15 | 4-K11 (M-2018), Cpx-Pl-SCH | WR | 8.954 | 44.21 | 0.1224 | 0.512642 ± 9 | 850 | 900 | 23.1 | 27.1 |
| | | Pl | 3.715 | 22.15 | 0.1014 | 0.512620 ± 15 | | | | |
| | | Amp | 9.093 | 38.64 | 0.1422 | 0.512712 ± 9 | | | | |
| 16 | (M-4), Grt-Amp-Cpx-Pl-AMT | WR | 12.8 | 69.3 | 0.1118 | 0.511126* | 3010 | 3030 | | 1.1 |
| 17 | 5-K11 (3-12/260), Cpx-Pl-Phl-SCH | WR | 4.729 | 25.00 | 0.1143 | 0.511050 ± 5 | 3200 | 3208 | –7.4 | 2.0 |
| | | Pl | 1.249 | 10.56 | 0.0715 | 0.510392 ± 8 | | | | |
| | | Cpx | 16.57 | 65.12 | 0.1538 | 0.511604 ± 7 | | | | |
| | | Phl | 5.734 | 30.41 | 0.1140 | 0.510981 ± 4 | | | | |
| 18 | 6-K11 (3-15/340), Grt-Cpx-Pl-ECR | WR | 6.506 | 40.82 | 0.0963 | 0.510879 ± 7 | 2933 | 2890 | –11.3 | 5.8 |
| | | Grt | 8.786 | 8.726 | 0.6085 | 0.516890 ± 9 | | | | |
| | | Pl | 0.459 | 3.575 | 0.0776 | 0.510695 ± 14 | | | | |
| | | CPx | 16.29 | 76.87 | 0.1281 | 0.511229 ± 2 | | | | |
| 19 | (ZP-12/230), Grt-Cpx-Pl-ECR | WR | 2.52 | 15.1 | 0.1008 | 0.510819* | 3129 | 3135 | –14.6 | 2.9 |
| 20 | (ZP-12/289), Grt-Cpx-Pl-ECR | WR | 21.1 | 95.2 | 0.1340 | 0.511422* | 3286 | 3258 | –10.1 | 1.3 |
| 21 | (ZP-15-340), Grt-Cpx-Pl-SCH | WR | 8.76 | 67.0 | 0.0789 | 0.510566* | 2907 | 2822 | –14.8 | 6.7 |
| 22 | (N-2/113), Grt-Amp-Cpx-Pl-AMT | WR | 7.82 | 34.9 | 0.1356 | 0.511638* | 2938 | 2965 | –4.8 | 4.9 |
| | | Grt | 2.14 | 1.92 | 0.6740 | 0.518231* | | | | |
| | | Pl-1 | 0.452 | 4.01 | 0.0681 | 0.510723* | | | | |
| | | Pl-2 | 0.394 | 2.57 | 0.0890 | 0.511042* | | | | |
| | | Amp | 10.7 | 43.5 | 0.1490 | 0.511719* | | | | |
| 23 | (Ud-78/88) | WR | 5.28 | 37.2 | 0.0857 | 0.512552* | 710 | – | – | –0.3 |
| 24 | (Ud-78/190) | WR | 6.79 | 54.3 | 0.0755 | 0.512526* | 690 | – | – | –0.6 |
| 25 | 11-230 | WR | 10.07 | 75.24 | 0.0809 | 0.512619 ± 2 | 600 | – | – | 1.1 |
| 26 | 13 | WR | 6.25 | 46.68 | 0.0808 | 0.512551 ± 12 | 700 | – | – | –0.2 |
| 27 | 16/4-270 | WR | 2.95 | 14.75 | 0.1211 | 0.512550 ± 12 | 990 | – | – | –0.8 |

**Table 1.** (Contd.)

| 1 | 2 | 3 | 4 | 5 | 6 | 7 | 8 | 9 | 10 | 11 |
|---|---|---|---|---|---|---|---|---|---|---|
| 28 | 1-S12 (10/3008) 6**, Cpx-Amp-Bt-GNS | WR | 5.424 | 38.717 | 0.0847 | 0.510648 ± 17 | 2940 | 3100 | –12.9 | –2.8 |
| | | Pl | 0.925 | 9.021 | 0.0620 | 0.510210 ± 15 | | | | |
| | | Cpx | 21.395 | 116.121 | 0.1114 | 0.511081 ± 12 | | | | |
| | | Bt | 11.055 | 62.352 | 0.1072 | 0.510807 ± 17 | | | | |
| | | Ap | 124.266 | 395.468 | 0.1900 | 0.511900 ± 14 | | | | |
| 29 | 11-S12 (2323/2073) 15**, Amp-GNS | WR | 2.402 | 12.402 | 0.1171 | 0.511212 ± 14 | 3041 | 3048 | –6.0 | 0.9 |
| | | Pl | 1.924 | 10.133 | 0.1148 | 0.511289 ± 19 | | | | |
| | | Bt | 4.402 | 18.906 | 0.1407 | 0.511785 ± 18 | | | | |
| | | Amp | 11.281 | 46.463 | 0.1468 | 0.512244 ± 12 | | | | |
| | | Ap | 86.823 | 268.551 | 0.1954 | 0.512315 ± 6 | | | | |
| 30 | 6-S12 (622/2744) 25**, Crd-Grt-Bt-GNS | WR | 4.268 | 23.436 | 0.1101 | 0.511411 ± 13 | 2549 | 2523 | –0.2 | 7.3 |
| | | Grt | 2.302 | 12.602 | 0.1104 | 0.511720 ± 18 | | | | |
| | | Pl | 0.398 | 2.620 | 0.0919 | 0.511467 ± 16 | | | | |
| | | Phl | 1.678 | 10.906 | 0.0930 | 0.511442 ± 13 | | | | |
| | | Ttn | 0.241 | 0.995 | 0.1466 | 0.512552 ± 25 | | | | |
| 31 | (AN-14), Grt-Bi-GNS | WR | 11.47 | 75.20 | 0.09221 | 0.510744 ± 10 | 3000 | 2973 | –11.0 | 4.8 |
| | | Grt | 6.626 | 18.95 | 0.21137 | 0.512276 ± 9 | | | | |
| | | Pl | 2.297 | 16.80 | 0.08265 | 0.510643 ± 9 | | | | |
| | | Mnz1 | 1.653(%) | 10.57(%) | 0.09451 | 0.510787 ± 8 | | | | |
| | | Mnz2 | 1.984(%) | 13.48(%) | 0.08901 | 0.510724 ± 9 | | | | |
| | | Mnz3 | 1.754(%) | 11.83(%) | 0.08965 | 0.510724 ± 7 | | | | |
| | | Mnz4 | 1.895(%) | 12.40(%) | 0.09239 | 0.510741 ± 7 | | | | |
| 32 | (AN-61), Opx-Cpx-Pl-GNS | WR | 1.518 | 10.83 | 0.08471 | 0.511212 ± 9 | 2274 | 1990 | –0.2 | 16.9 |
| | | Pl | 0.466 | 5.679 | 0.04961 | 0.510773 ± 6 | | | | |
| | | Cpx | 3.691 | 21.28 | 0.10486 | 0.511455 ± 5 | | | | |
| | | Ap | 321.9 | 1775.4 | 0.10961 | 0.511533 ± 8 | | | | |
| | | Ilm | 1.365 | 9.393 | 0.08787 | 0.511267 ± 9 | | | | |
| 33 | (885-2), DDY | WR | 4.86 | 19.4 | 0.15194 | 0.512336 ± 9 | 2007 | 2004 | | |
| 34 | (AN-82), Bi-Cpx-GNS | WR | 5.942 | 34.52 | 0.10405 | 0.511481 ± 10 | 2313 | 2316 | 0.2 | 4.8 |
| | | Grt | 9.227 | 11.58 | 0.48163 | 0.516245 ± 10 | | | | |
| | | Pl | 5.048 | 44.76 | 0.07798 | 0.511156 ± 8 | | | | |
| 35 | (AN-91), Bi-Cpx-GNS | WR | 6.226 | 34.08 | 0.11043 | 0.511517 ± 10 | 2410 | 2300 | –0.6 | 1.4 |
| | | Grt | 11.84 | 38.01 | 0.18825 | 0.512498 ± 11 | | | | |
| | | Pl | 2.720 | 19.05 | 0.08631 | 0.511229 ± 11 | | | | |
| | | Ap | 450.7 | 1111.9 | 0.24503 | 0.513216 ± 17 | | | | |
| | | Mnz | 2.640(%) | 16.58(%) | 0.09626 | 0.511348 ± 8 | | | | |

Notes: (*) Analytical accuracy is not indicated in the work by Neimark et al. (1992). (**) Shown in brackets are borehole numbers as in Fig. 4/sampling depth. Time $T_2$ is accepted according to ages of granulite metamorphism (Sm–Nd mineral isochrons, accepted dates, Table 2). Time $T_1$ for the Daldyn terrane is 3.1 Ga accepted based on Sm–Nd whole-rock isochron (Spiridonov et al., 1993), U–Pb zircon date at the upper intercept of discordia, Sample 6K11(3-15/340), this work, Table 4 and after Rosen et al. (2000); for the Magan and Markha terranes, $T_1$ = 2.8 and 2.5 Ga, respectively, U–Pb zircon dates, this work, samples 10-S12(1002/2703) and 8-S12 (706/3100), Table 4; for the Birekte terrane, $T_1$ = 2.3 Ga, U–Pb zircon date (1.97 Ga), T(Nd)DM of 2.32 Ga (Rosen et al., 2000).
Symbols for minerals and rocks hereinafter: (Amp) amphibole, (Ap) apatite, (Bt) biotite, (Cord) cordierite, (Cpx) clinopyroxene, (Grt) garnet, (Ilm) ilmenite, (Mic) micas, (Mnz) monazite, (Opx) orthopyroxene, (Phl) phlogopite, (Pl) plagioclase, (Sil) sillimanite, (Ttn) titanite, (WR) whole rock, (AMT) amphibolite, (DDY) dolerite from dike, (ECR) eclogite-like rock, (GNS) gneiss, (GRN) granite, (SCH) crystalline schist; combination of symbols designates the rock type, e.g., Crd-Grt-Bt-GNS means cordierite-garnet-biotite gneiss.
Sampling localities. **Crustal xenoliths in kimberlites** (nos. 1–22). **Markha terrane**: (1–4) Nakyn field, Botuoba pipe, (5–9) Daldyn field: (5–7) Udachnaya pipe, (8) Dal'nyaya pipe, (9) Zarnitsa pipe; (10–13) Alakit field, Satykan pipe; (14–16) **Magan terrane**, Mir field, Mir pipe; (17–22) **Daldyn terrane**, Muna field: (17–21), Zapolyarnaya pipe, (22) Novinka pipe. **Including kimberlites**: (23, 24) Udachnaya pipe, Daldyn field, (25) Inter pipe, Mir field, (26) Zarnitsa pipe, Daldyn field, (27) Botuoba pipe, Nakyn field. **Boreholes** (nos. 28–30): (28) Markha terrane, (29, 30) Magan terrane. **Outcrops in the Anabar shield** (nos. 31–35): (31–33) Daldyn terrane, (34, 35). Birekte terrane.

**Table 2.** Interpreted results of the Sm–Nd isotope analysis of samples from crustal xenoliths in kimberlites, drill cores, and outcrops

| No. | Sample number, analytical (original), rock | Probable isochrons based on combinations of minerals | | | |
|---|---|---|---|---|---|
| | | minerals | Ma | εNd(0) | MSWD |
| 1 | 8-VK4 | WR-Grt-Pl | **1760 ± 40*** | –24.0 | 0.03 |
| 2 | 12-VK4 | WR-Grt-Pl | **1831 ± 13** | –16.2 | 0.0014 |
| | | WR-Grt-PL-Amp | 1827 ± 44 | | 4.8 |
| 3 | 13-VK4 | WR-Grt-PL | **1834 ± 13** | –11.7 | 0.037 |
| | | WR-Grt-PL-Bt-Cpx | 1790 ± 220 | | 379 |
| 4 | 14-VK4 | WR-Grt-Bt | 1785 ± 200 | –24.0 | 6.54 |
| | | WR-Grt-Pl-Bt | 1769 ± 140 | | 33.3 |
| | | WR-Grt | **1775 ± 17** | | – |
| 5 | 1-K11 (U-2295) | WR-Grt-Pl-Cpx | 1612 ± 730 | –26.0 | 443 |
| | | WR-Grt | 1355 ± 25 | | – |
| | | WR-Cpx | 2190 ± 120 | | – |
| | | Pl-Grt | 1628 ± 19 | | – |
| | | Grt-Cpx | **1666 ± 21** | | – |
| 6 | U-2030a | Grt-Cpx | **1756 ± 6** | –7.9 | |
| 7 | 2-K11 (D-40) | all points | 1707 ± 120 | –25.7 | 15.4 |
| | | Wr-Grt-Cpx | 1716 ± 210 | | 2.01 |
| | | WR-Gar | **1709 ± 19** | | – |
| 8 | 7-K11 (Zr-14) | WR-Grt-Pl | **1627 ± 18** | –12.3 | 0.964 |
| 9 | 8-K11 (S-45) | WR-Grt-Pl-Fl | 1802 ± 470 | –20.0 | 95.3 |
| | | WR-Grt | **1684 ± 30** | | – |
| | | Grt-Pl-Fl | 1850 ± 260 | | 2.82 |
| 10 | 9-K11 (S-84) | WR-Grt-Pl-Fl | 1837 ± 180 | –24.3 | 6.47 |
| | | WR-Grt-Fl | **1862 ± 37** | | 0.932 |
| | | WR-Grt | 1850 ± 44 | | – |
| 11 | 10-K11 (S-86) | WR-Grt-Pl-Fl | 1860 ± 190 | –21.2 | 1.88 |
| | | WR-Grt-Pl | **1840 ± 70** | | 0.585 |
| 12 | 11-K11 (S-99/463) | WR-Grt-Pl-Am-Phl | **1881 ± 30** | –21.1 | 1.03 |
| 13 | 5-K11 (Z-12/260) | WR-Pl-Fl-Cpx | **2233 ± 360** | –31.0 | 5.82 |
| 14 | 6-K11 (Z-15/340) | WR-Grt-Pl-Cpx | 1781 ± 49 | –34.3 | 4.92 |
| | | WR-Grt-Cpx | **1787 ± 14** | | 1.63 |
| | | Grt-Pl-Cpx | 1781 ± 200 | | 9.57 |
| 15 | N-2/113 | Grt-(Pl-1)-Amp | **1884 ± 5** | –19.5 | 0.61 |
| 16 | 1-S12 (10/3008) 6 | all points | 1949 ± 570 | –38.8 | 76.5 |
| | | WR-Pl-Bt-Ap | 1948 ± 540 | | 38 |
| | | WR-Ap | **1808 ± 54** | | – |
| | | Pl-Bt-Ap | 2006 ± 44 | | 0.0001 |
| 17 | 11-S12 (2323/2073) 15 | all points | 2092 ± 2200 | –27.8 | 450 |
| | | WR-Ap | **2137 ± 75** | | – |
| | | WR-Pl-Ap | 2029 ± 2300 | | 32.5 |
| | | WR-Pl-Bt-Ap | 2020 ± 1300 | | 98.4 |
| 18 | 6-S12 (622/2744) 25 | all points | 3077 ± 2200 | –23.9 | 208 |
| | | Pl-Phl-Ti | 3067 ± 1500 | | 6.27 |
| 19 | (AN-14) | all points | **1938 ± 30** | –36.9 | 0.97 |
| 20 | (AN-61) | WR-Pl-Cpx-Ap-Ilm | **1905 ± 70** | –26.7 | 0.98 |
| 21 | (AN-82) | WR-Grt-Pl | **1916 ± 3** | –22.6 | 0.06 |
| 22 | (AN-91) | WR-Grt-Pl-Ap-Mnz | **1906 ± 14** | –21.9 | 0.34 |

Note: (*) Values accepted for further discussion (other explanations in Table 1). Sampling localities. **Crustal xenoliths in kimberlites** (nos. 1–15). **Markha terrane**: (1–4) **Nakyn field**, Botuoba pipe, (5–8) **Daldyn field**: (5, 6) Udachnaya pipe, (7) Dal'nyaya pipe, (8) Zarnitsa pipe; (9–12) **Alakit field**, Satykan pipe; (13–15) **Daldyn terrane**, Muna field: (13, 14) Zapolyarnaya pipe, (15) Novinka pipe. **Boreholes** (nos. 16–18): (16) Markha terrane, (17, 18) Magan terrane. **Outcrops in the Anabar shield** (nos. 18–21): (18, 19) Daldyn terrane, (20, 21) Birekte terrane.

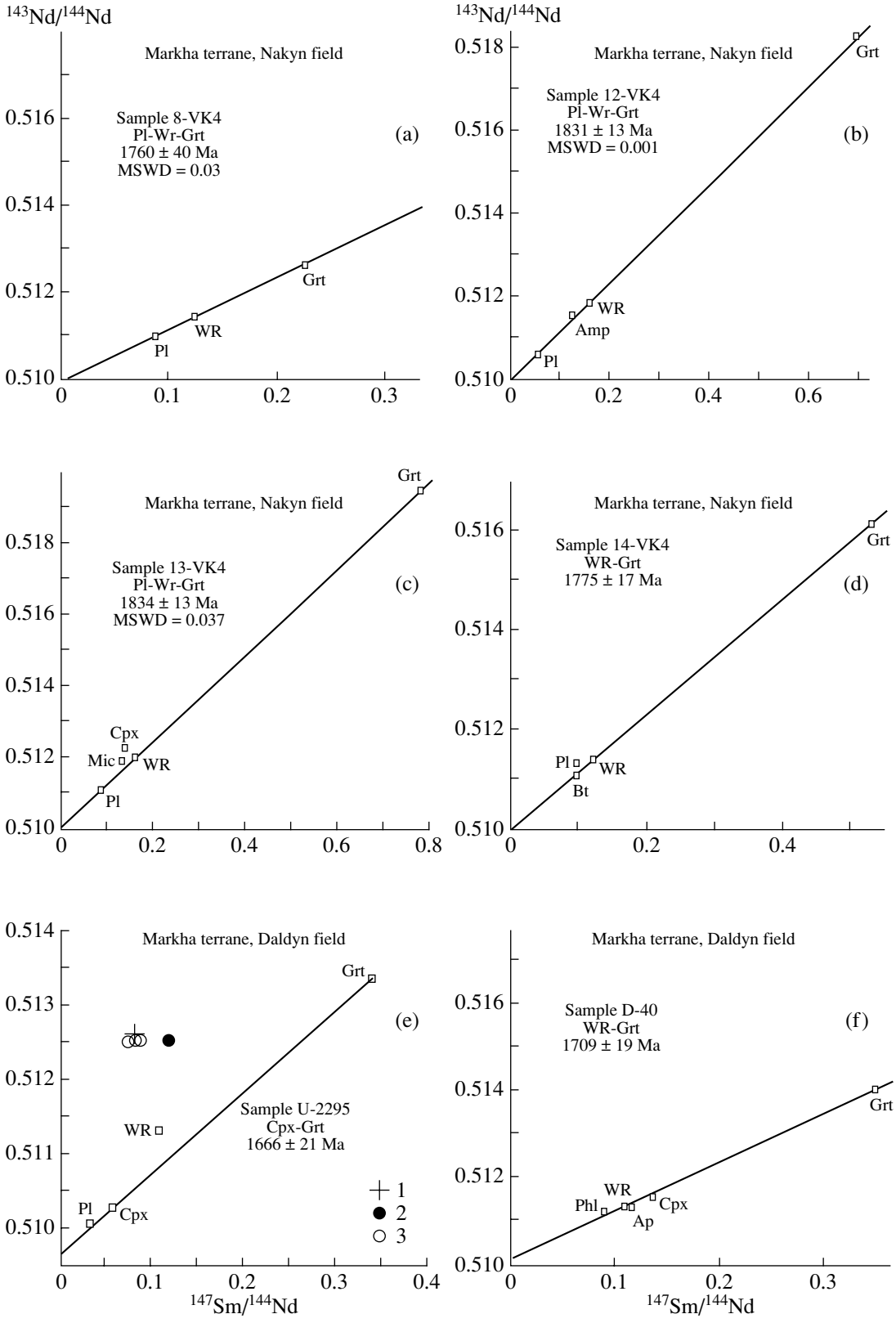


**Fig. 6.** Sm–Nd isochron diagrams (a–l) (whole rock–minerals) for representative crustal xenoliths from kimberlites (Table 2, accepted values); analytical data for xenoliths from Mirnyi (1), Nakyn (2) and Daldyn (3) fields are presented in Table 1 (symbol sizes substantially exceed the measurement error).

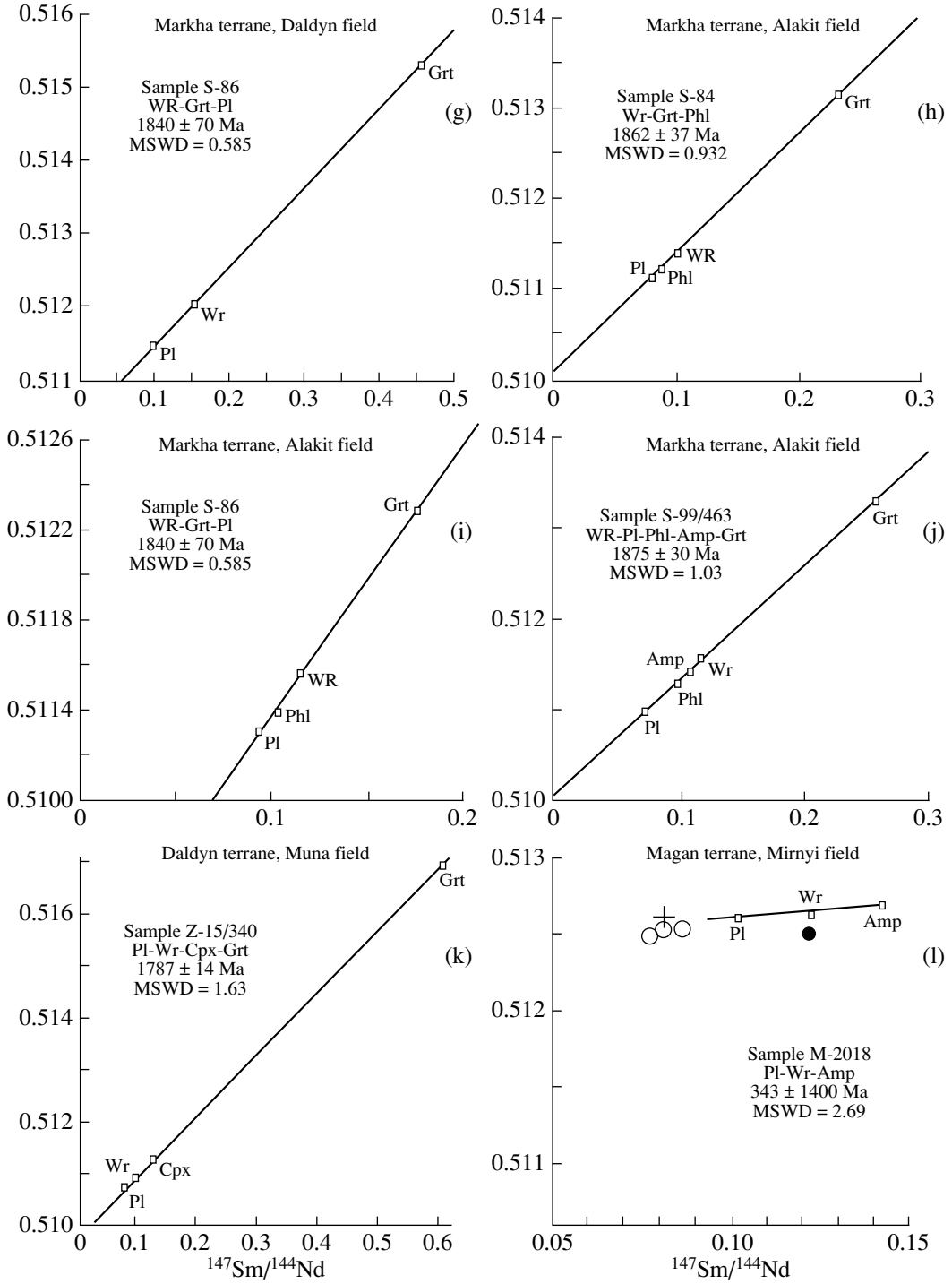


**Fig. 6.** (Contd.)

izes only the time of kimberlite magmatism, but not formation of a original substratum.

The Sm–Nd isotopic diagram for rocks from the Northeast Siberian craton demonstrates that evolutionary lines of the Daldyn terrane terminate in the area corresponding to the mantle source that is approximately 3.1 Ga old (Fig. 7). Rocks of the Magan terrane separated slightly later from the mantle. The Markha and Birekte granite–greenstone terranes show significantly scattered ages, and this can be explained by their heterogeneity: dominant plagiogranites enclose here local greenstone belts and their age relations are unclear. The granite terrane was separated from mantle source probably during the period of 2.90 to 2.25 Ga and the second

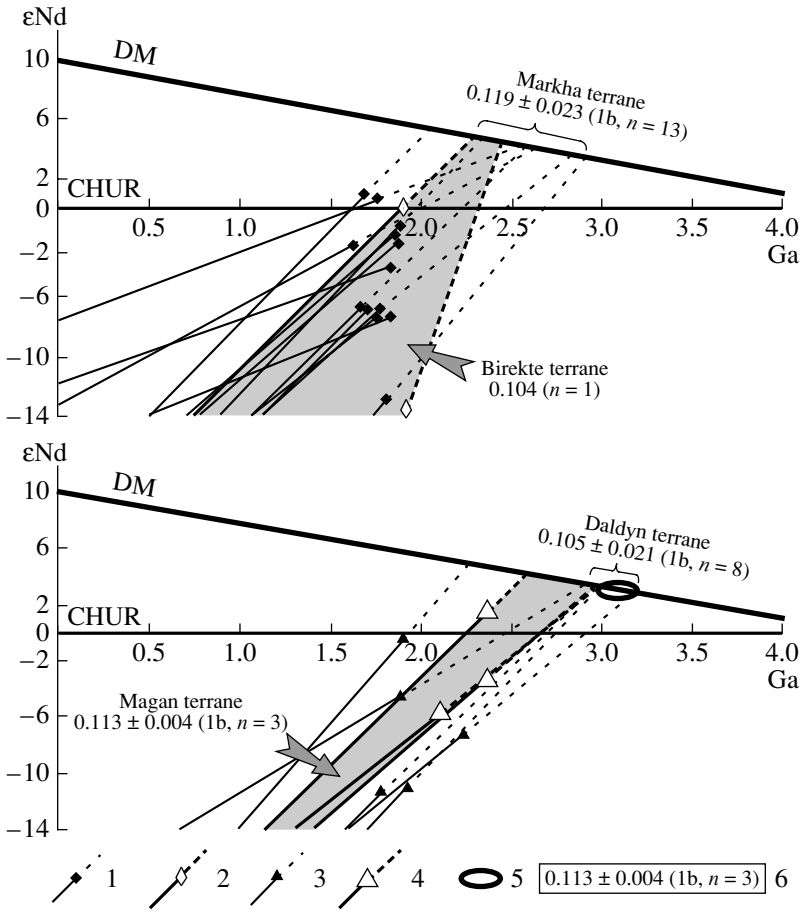


**Fig. 7.** Sm–Nd isotope evolution diagram for rocks of the Northeast Siberian craton:
(1–4) evolution curves and time of the metamorphic system closure according to Sm–Nd mineral isochrons and zircon dates, in part for (1) Markha, (2) Birekte, (3) Daldyn and (4) Magan terranes; (5) age of source for the Daldyn terrane metavolcanics, Sm–Nd whole-rock isochrons (Spiridonov et al., 1993); (6) average $^{147}Sm/^{144}Nd$ value, statistical deviation, number of analyses (except for two values exceeding value of 0.16 that is close to parameter accepted for chondrite uniform reservoir); (DM) evolution line of depleted mantle; (CHUR) chondrite uniform reservoir.

terrane at the end of this period. Average $^{147}Sm/^{144}Nd$ ratios of 0.104 to 0.119 obtained for examined rocks characterize the terrane complexes as a mature continental crust, for which this parameter is accepted to be 0.112 (Taylor and McLennan, 1985).

Periodicity in granulite metamorphism during continental collision is evident from distribution of isochron dates (Fig. 8). The examined mineral parageneses of garnet, two pyroxene, phlogopite, and plagioclase, which is typical of most samples, corresponds largely to the granulite facies. Isochrons based on these minerals suggest three events of granulite metamorphism in the period of 2.2 to 1.6 Ga, which are presumably caused by episodes of crustal thickening during intermittent thrusting of terranes in response to collision. These episodes were probably separated by epochs of the local collision prism collapse.

Comparison of model Sm–Nd ages (data on whole-rock samples) and dates estimated based on mineral isochrons elucidates age relations of terrane rocks with superimposed metamorphism reflecting paroxysm of collision-related compression and crustal thickening (Fig. 9). Accretion of collision prism likely developed in the step-by-step manner from the east westward (in present-day coordinates). The Daldyn terrane collided first with the Markha terrane and then, being coupled, they were thrust westward onto the Magan terrane. Later on, they were overridden by the Birekte terrane. During the local collapse after the first collision stage 2.2–2.1 Ga ago, the Daldyn and Markha terranes were probably intruded by mafic rocks (present-day crystalline schists) with model T(NdDM)(2st) ages of 1990 and 1960 Ma, respectively. The dolerite dike with T(NdDM)(2st) = 2004 Ma intruded the Kotuikan suture at that time as well. Anomalously old T(NdDM)(2st) values of 3204 and 3100 Ma estimated for the Markha terrane are explainable in terms of terrane heterogeneity mentioned above.

**Results of the Rb–Sr dating and their interpretation.** The results are presented in Table 3. Initial Sr-iso-

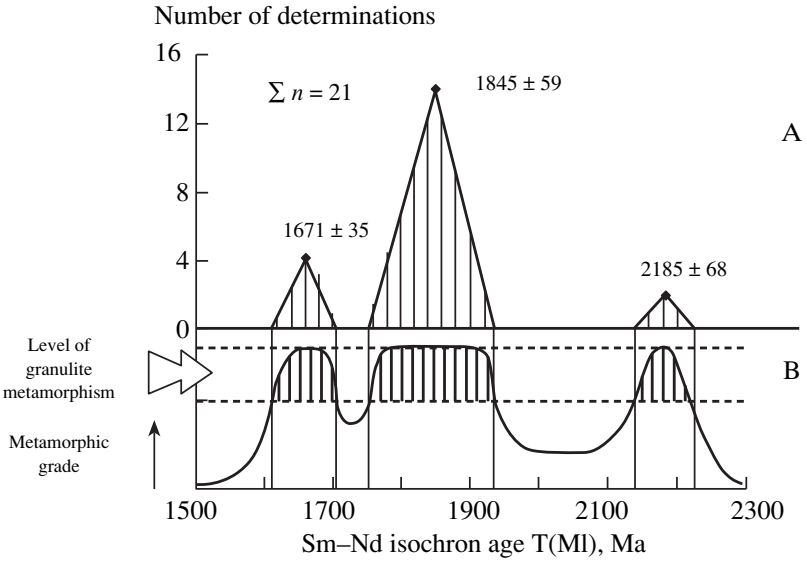


**Fig. 8.** Diagram demonstrating distribution of dates (Sm–Nd mineral isochrons) and periodicity of granulite metamorphism in the course of continental collision.

(A) Average values on Sm–Nd mineral isochron ages (Ma) and standard deviations, the triangle base width corresponds to values scattering. (B) Curve qualitatively depicting episodes of granulite metamorphism responsible for isotopic equilibration of examined minerals.

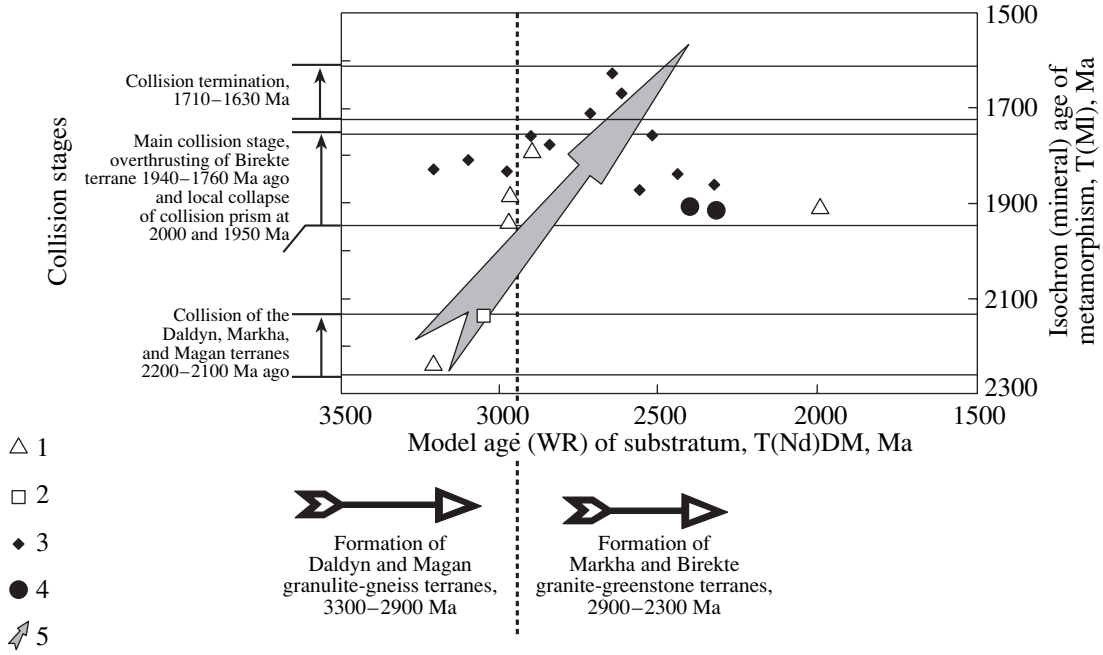


**Fig. 9.** Relation between Sm–Nd model ages estimated based on whole-rock dating results and mineral isochrons.

(1–4) examined samples from (1) Daldyn, (2) Magan, (3) Markha and (4) Birekte terranes; (5) secular trend of collision-related metamorphic events.

tope ratio (IR) range considerably from 0.6975 to 0.7195, being equal in average to 0.70612 ± 0.00143 (1σ, $n$ = 5) for metamafites (crystalline schists) and to 0.7074 ± 0.0087 (1σ, $n$ = 10) for felsic rocks (gneisses), thus formally suggesting a substantial crustal maturity. The Sm–Nd isotopic diagram shows that protoliths (presumably, metabasalts) experienced probably interaction with seawater and that some felsic rocks correspond in isotopic parameters to the continental crust (Fig. 10).

**Table 3.** Results of the Rb–Sr isotopic analysis of crustal xenoliths from kimberlites and drill-core samples

| No. | Sample number, analytical (original), rock | Material | Rb, μg/g | Sr, μg/g | $^{87}Rb/^{86}Sr$ | $^{87}Sr/^{86}Sr$ | Isochron interpretation, *T*, Ma | IR | MSWD |
|---|---|---|---|---|---|---|---|---|---|
| 1 | 14-VK4, Bt-Pl-Grt-SCH | WR | 23.45 | 167.8 | 0.4043 | 0.715019 ± 18 | WR-Bt: 1466 ± 8** | 0.7065 ± 2 | |
| | | Bt | 169.7 | 59.64 | 8.3657 | 0.882510 ± 7 | | | |
| 2 | 2-K11 (D-40), Gt-Cpx-Phl-SCH | WR | 46.63 | 319.0 | 0.4227 | 0.713770 ± 6 | WR-Phl: 1347 ± 7 | 0.7056 ± 2 | |
| | | Phl | 518.2 | 117.7 | 13.03 | 0.957223 ± 6 | | | |
| 3 | 8-K11 (S-45), Phl-Gt-Pl-GNS | WR | 128.0 | 661.4 | 0.5601 | 0.721403 ± 10 | WR-Phl: 2000 ± 12 | 0.7053 ± 4 | |
| | | Phl | 685.1 | 306.7 | 6.572 | 0.894635 ± 11 | | | |
| 4 | 9-K11 (S-84), Grt-Pl-Phl-GNS | WR | 200.7 | 1161 | 0.5001 | 0.720873 ± 9 | WR-Phl: 1541 ± 10 | 0.7098 ± 2 | |
| | | Phl | 730.6 | 315.8 | 6.784 | 0.859881 ± 8 | | | |
| 5 | 10-K11 (S-86), Grt-Pl-Phl-SCH | WR | 166.3 | 1436 | 0.3350 | 0.716157 ± 6 | WR-Phl: 1850 ± 13 | 0.7072 ± 2 | |
| | | Phl | 575.7 | 598.7 | 2.7991 | 0.781761 ± 6 | | | |
| 6 | 11-K11 (S-99/463), Grt-Pl-Amp-Phl-GNS | WR | 40.64 | 1112 | 0.1055 | 0.709959 ± 9 | WR-Phl: 1563 ± 9 | 0.7076 ± 4 | |
| | | Phl | 455.4 | 242.7 | 5.496 | 0.845554 ± 7 | | | |
| 7 | 3-K11 (M-2017), Cpx-Pl-Ph-SCH | WR | 25.39 | 202.3 | 0.3628 | 0.712893 ± 9 | WR-Phl: 1732 ± 11 | 0.7039 ± 4 | |
| | | Phl | 123.3 | 64.69 | 5.585 | 0.842964 ± 12 | | | |
| 8 | 5-K11 (Z-12/260), Cpx-Pl-Phl-SCH | WR | 37.86 | 2000 | 0.0547 | 0.708693 ± 5 | WR-Phl: 1608 ± 39 | 0.7074 ± 2 | |
| | | Phl | 94.33 | 455.0 | 0.5999 | 0.721287 ± 12 | | | |
| 9 | 7-S12 (703/2590) 1*, Bt-Amp-GNS | WR | 10.1 | 158.7 | 0.1902 | 0.71069 ± 11 | WR-Amp: 628 ± 39 | 0.7089 ± 4 | |
| | | Pl | 2.7 | 427.4 | 0.0189 | 0.70529 ± 15 | Pl-Amp: 880 ± 32 | 0.7050 ± 3 | |
| | | Amp | 16.4 | 45 | 1.090 | 0.71875 ± 16 | WR-Pl-Amp: 797 ± 2700 | 0.7066 ± 246 | 194 |
| 10 | 8-S12 (706/3100) 2, Crd-Opx-GNS | WR | 92.8 | 394 | 0.7008 | 0.71979 ± 29 | WR-Bt: 2204 ± 11 | 0.6975 ± 4 | |
| | | Pl | 86.7 | 295.4 | 0.8743 | 0.73413 ± 14 | WR-Pl-Bt: 2195 ± 230 | 0.7017 ± 634 | |
| | | Bt | 378.3 | 36.5 | 31.294 | 1.6926 ± 4 | | | |

**Table 3.** (Contd.)

| No. | Sample number, analytical (original), rock | Material | Rb, μg/g | Sr, μg/g | $^{87}Rb/^{86}Sr$ | $^{87}Sr/^{86}Sr$ | Isochron interpretation, *T*, Ma | IR | MSWD |
|---|---|---|---|---|---|---|---|---|---|
| 11 | 5-S12 (622/2742) 25, Crd-Ga-Bt-GNS | WR | 140.4 | 108.5 | 3.852 | 0.82675 ± 33 | WR-Bt: 1948 ± 11 | 0.7195 ± 9 | |
| | | Pl | 61.3 | 117.6 | 1.555 | 0.75699 ± C12 | WR-Pl-Bt: 1954 ± 130 | 0.714 ± 3 | 180 |
| | | Bt | 315.8 | 21.9 | 43.15 | 1.92977 ± C12 | | | |
| 12 | 10-S12 (1002/2703) 7, Bt-GRN-CTC | WR | 63.6 | 836 | 0.2265 | 0.71068 ± 3 | 1420 | 0.706*** | |
| 13 | 12-S12 (15502/2199) 12, Bt-Opx-Pl-GNS | WR | 58.2 | 685.4 | 0.2530 | 0.71315 ± 13 | WR-Phl: 1753 ± 9 | 0.6949 ± 3 | |
| | | Pl | 24.7 | 429 | 0.1717 | 0.70894 ± 13 | WR-Pl = Phl: 1733 ± 430 | 0.699 ± 62 | 1490 |
| | | Phl | 571.2 | 98 | 17.37 | 1.1326 ± 2 | | | |
| | | Amp | 362.5 | 109.4 | 9.899 | 0.70340 ± 7 | | | |
| 14 | 2-S12 (100/2020) 20, Sil-2Mic-Pl-GNS | WR | 28.3 | 95.2 | 0.8882 | 0.74539 ± 9 | WR-Phl: 1783 ± 8.8 | 0.7226 ± 4 | |
| | | Pl | 2.8 | 11.5 | 0.7362 | 0.73088 ± 29 | Pl-Phl: 1796 ± 8.9 | 0.7119 ± 4 | |
| | | Phl | 447.1 | 11.5 | 56.69 | 2.1761 ± 7 | WR-Pl-Phl: 1789 ± 150 | 0.717 ± 73 | 1520 |
| 15 | 3-S12 (100/2022) 20, Bt-Pl-GNS | WR | 21.8 | 762.6 | 0.0850 | 0.70448 ± 5 | WR-Phl: 1967 ± 9.8 | 0.70207 ± 21 | |
| | | Pl | 9.5 | 672 | 0.0423 | 0.70302 ± 8 | WR-Pl-Phl: 1968 ± 64 | 0.7019 ± 16 | |
| | | Phl | 247.9 | 58.8 | 12.61 | 1.0594 ± 4 | | | |
| 16 | 4-S12 (576/2033) 23, Mic-Pl-GNS | WR | 21.8 | 443.5 | 0.1464 | 0.70837 ± 9 | WR-Bt: 1024 ± 6.2 | 0.7062 ± 2 | |
| | | Pl | 0.37 | 21.6 | 0.0514 | 0.70469 ± 30 | WR-Pl-Bt: 1033 ± 200 | 0.7056 ± 10 | 123 |
| | | Amp | 186.3 | 197.7 | 2.807 | 0.78962 ± 21 | | | |
| | | Bt | 359.2 | 119.7 | 8.945 | 0.83725 ± 37 | | | |
| 17 | 13-S12 (20702/2201) 31, Amp-GRN | Pl | 35.3 | 1670 | 0.0628 | 0.70376 ± 8 | Pl-Amp: 1414 ± 320 | 0.70248 ± 46 | |
| | | Amp | 9 | 211.7 | 0.1264 | 0.70505 ± 12 | | | |

Note: (*) Shown in brackets are borehole numbers as in Fig. 4/sampling depth; (**) values accepted for further discussion; (***) most probable value (other explanations in Table 1). Sampling localities. **Crustal xenoliths in kimberlites** (nos. 1–8). (1–6) **Markha terrane**: (1) **Nakyn field**, Botuoba pipe, (2) **Daldyn field**, Dal'nyaya pipe, (3–6) Alakit field, Satykan pipe, (7) Magan terrane, Mir field, (8) Daldyn terrane, Muna field, Zapolyarnaya pipe. **Boreholes** (nos. 9–16). (9–11) Markha terrane, (12–16) Magan terrane.

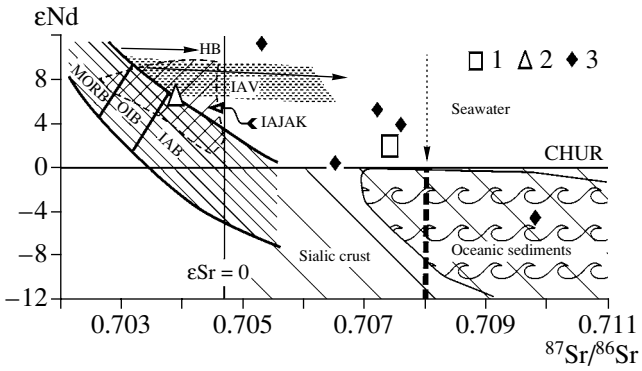


**Fig. 10.** εNd–$^{87}Sr/^{86}Sr$ diagram (De Paolo and Wasserburg, 1979; Anderson, 1989; Rolinson, 1994, with modifications) illustrating evolution of mantle melts and seawater influence: (1–3) samples (mafic crystalline schists mostly and only two felsic gneisses with maximal $^{87}Sr/^{86}Sr$ values) from (1) Daldyn, (2) Magan and (3) Markha terranes; abbreviations in figure: (MORB) mid-ocean ridge basalts, (IAB) island-arc basalts, (IAV) island-arc volcanics, (OIB) oceanic island basalts, (HB) hidrated basalts, (IAJAK) hydrated basalts and island-arc migmatites of Japan, Alaska and the Kurile Islands (after Govorov et al., 2005).

By geochronological interpretation of analytical results, we focused attention on two-point isochrons plotted for whole rock–magnesian mica pairs, which are most representative in terms of relevant elements concentrations. Comparing these and Sm–Nd isochrons characterizing the same samples (Fig. 11), one can see that interval of Rb–Sr dates is extended toward younger ages. This is explainable by closure of Rb–Sr isotopic systems in corresponding minerals under lower crystallization temperatures (≈300°C) in the course of gradual cooling of collision prism. Dates (1850 Ma) coinciding within the accuracy limits are established for single sample 10-K11 (C-86), and this is probably indicative of a rapid cooling during intense exhumation and erosion of local domain. In five of seven cases, Rb–Sr ages are equal to about 0.8 of parallel Sm–Nd dates with correlation coefficient $R \approx 0.90$ that means the regular delay (approximately by 300 m.y.) in closure of Rb–Sr isotopic systems during gradual cooling. In one of the samples 8-K11(C-45), the Sm–Nd and Rb–Sr ages are 1684 and 2000 Ma, respectively. The older Rb–Sr age probably indicates in this case the Rb removal from the melt during partial melting of anatectic granites. The observable lag of Rb–Sr isotopic systems is related to different closure temperatures, while the time span of 300 m.y. established in the Northeast Siberian craton is probably determined by the long-term standing of a relic orogenic structure, when temperature in the middle crust was approximately 300°C, i.e., comparable with the temperature in the crust basal part beneath present-day old platforms.

Thus, the considered age estimates are internally coordinated and represent a functional database for correlation of dated events within the entire Siberian craton.

## CONCLUSIONS

The Kotuikan and Billyakh sutures (collision zones) incorporating fragments of island-arc complexes determine structure of the Anabar collision system. Prior to accretion of the craton, they probably corresponded to parts of oceanic basin. It is assumed that microcontinents that existed in that basin have been amalgamated in the course of collision to form present-day terranes in mosaic structure of the craton. Crustal relicts thickened at the time of collision thrusting are locally preserved in the present-day structure.

Crystalline schists, gneisses, and granitoids are dated by Sm–Nd and Rb–Sr methods. The obtained results characterize the age of metamorphism, subse-

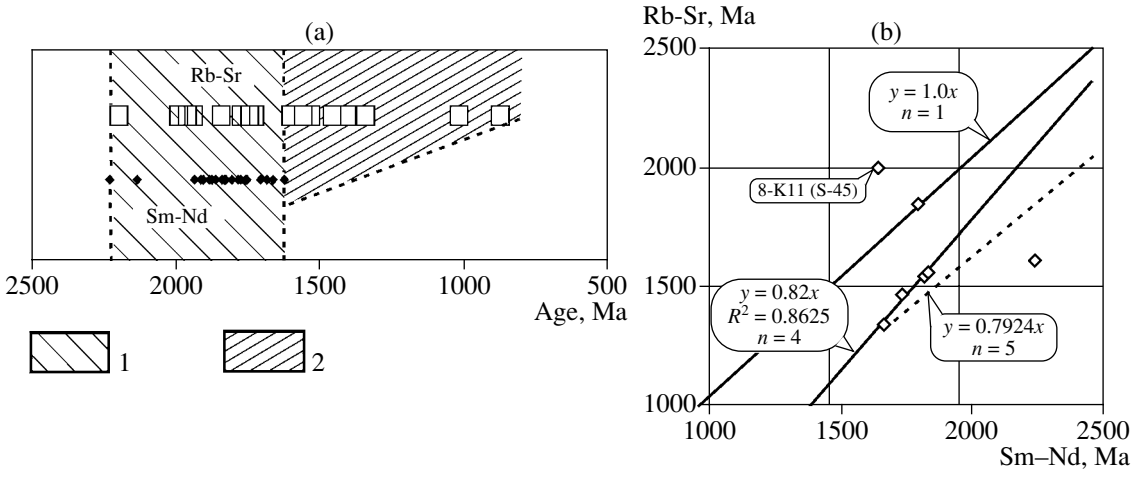


**Fig. 11.** Correlation between Rb–Sr and Sm–Nd mineral isochron dates; (a) composite diagram for all dates demonstrating (1) coincidence area and (2) area of relatively lowered Rb–Sr values; (b) covariation of Rb–Sr and Sm–Nd dates obtained for the same samples (symbol sizes exceed the analytical errors).

quent cooling (mineral isochron ages), and presumable time of crustal material separation from depleted mantle (the Sm–Nd model ages). Three groups of age values defined for collision-related metamorphism and mafic magmatism characterize presumably three collision epochs in the periods of 2200–2100, 1940–1760, and 1710–1630 Ma. Generation of mafic magmas derived from 2000- to 1960-Ma-old substratum was related to adiabatic ascent of asthenosphere up to the lower crust base during the local collapse of collision prism. Comparative analysis of Sm–Nd and Rb–Sr isochron dates obtained for the same samples of metamorphic rocks shows that the system cooling from 700 to ≈300°C lasted approximately 300 m.y. and substantially postdated the collision-related metamorphism and granite formation.

Over the entire Siberian craton, collision events were to a certain extent concurrent to formation of the Anabar collision prism. The presented materials suggest that they were more diverse and durable than it was thought before.

The Anabar collision system was formed during three separate periods (episodes) of collision. Each of collision stages superimposed in the system lasted approximately 100 m.y., being approximately comparable in duration and processes of petrogenesis with one collision stage comprehensively described in southern Finland (Nironen et al., 2000). The collision systems of such a long development were unknown so far.

Accretionary tectonics in Siberian craton presumably resulted in formation of a giant collision-related orogenic system of the Himalayan type. This orogen underlain by abnormally thick crust was eroded up to the state of granite layer denudation in places, as it is clearly evident in the Anabar shield (Rosen and Fedorovskii, 2001). The peneplain formed 1.65 Ga ago was subsequently buried under gently dipping Meso- to Neoproterozoic (Riphean) platform cover.

## ACKNOWLEDGMENTS

We are grateful to E.V. Bibikova and E.V. Sklyarov, who thoroughly reviewed the manuscript with valuable comments, which are taken into account in the final version manuscript. The work was supported by the Russian Foundation for Basic Research, project nos. 02-05-64779 and 03-05-64736.

Reviewers E.V. Bibikova and E.V. Sklyarov

## REFERENCES

1. A. M. Akhmedov, E. V. Bibikova, Yu. B. Bogdanov, et al., "Resolution of the Third All-Russian Meeting "General Problems of Precambrian Stratigraphy," Stratigr. Geol. Korrelyatsiya **9** (3), 101–106 (2001) [Stratigr. Geol. Correlation **9**, 304–308 (2001)].
2. D. L. Anderson, *Theory of the Earth* (Balckwell, Brookline, 1989).
3. E. F. Baxter, J. J. Ague, and D. J. De Paolo, "Prograde Temperature–Time Evolution of the Barrovian Type-Locality Constrained by Sm/Nd Garnet Ages from Glen Clova, Scotland," J. Geol. Soc. London **159**, 71–82 (2002).
4. O. A. Bogatikov, V. A. Kononova, Yu. Yu. Golubeva, et al., "Variations in Chemical and Isotopic Compositions of the Yakut Kimberlites and Their Causes," Geokhimiya, **42**, 915–939 (2004) [Geochemistry International **42**, 797–821 (2004)].
5. J. H. Davies and F. von Blankenburg, "Slab Break Off: A Model of Lithosphere Detachment and Its Test in the Magmatism and Deformation of Collision Orogen," Earth and Planet. Sci. Lett. **129**, 85–102 (1995).
6. *Classification and Nomenclature of Metamorphic Rocks, A Guidebook*, Ed. by N.L. Dobretsov, O.A. Bogatikov, and O.M. Rosen (OIGGM, Novosibirsk, 1992) [in Russian].
7. D. J. De Paolo and G. J. Wasserburg, "Petrogenic Mixing Models and Nd–Sm Isotopic Patterns," Geochim. et Cosmochim. Acta **43**, 615–627 (1979).
8. C. C. Diaconescu and J. H. Knapp, "Role of a Phase-Change Moho in Stabilization and Preservation of the Southern Uralide Orogen, Russia," Geophys. Monograph **132**, 67–82 (2002).
9. A. N. Didenko, I. K. Kozakov, E. V. Bibikova, et al., "Paleoproterozoic Granites of the Sharyzhalgai Block, Siberian Craton: Paleomagnetism and Geodynamic Inferences," Dokl. Akad. Nauk **390**, 368–373 (2003) [Doklady Earth Sciences **390**, 510–515 (2003)].
10. N. L. Dobretsov, A. G. Kirdyashkin, and A. A. Kirdyashkin, *Deep-Level Geodynamics* (RAN GEO, Novosibirsk, 2001) [in Russian].
11. T. V. Donskaya, D. P. Gladkochub, V. P. Kovach, and A. M. Mazukabzov, "Petrogenesis of Early Proterozoic Postcollision Granitoids in the Southern Siberian Craton," Petrologiya **13**, 253–279 (2005) [Petrology **13**, 229–252 (2005)].
12. K. N. Egorov, L. V. Solov'eva, V. P. Kovach, et al., "Mineralogical and Isotope-Geochemical Characteristics of Diamondiferous Lamproites of the Sayan Region," Dokl. Akad. Nauk **403**, 373–377 (2005) [Doklady Earth Sciences **403A**, 861–865 (2005)].
13. P. C. England and B. Thompson, "Pressure–Temperature–Time Paths of Regional Metamorphism," J. Petrol. **25**, 894–955 (1984).
14. B. R. Frost, O. V. Avchenko, K. R. Chamberlain, and C. D. Frost, "Evidence for Extensive Proterozoic Remobilization of the Aldan Shield and Implications for Proterozoic Plate Tectonic Reconstructions of Siberia and Laurentia," Precambrian Res. **89** (1–2), 1–23 (1998).
15. R. A. Gafarov, A. M. Leites, V. S. Fedorovskii, et al., "Tectonic Zoning of the Siberian Platform Basement and Successive Formation of the Continental Crust," Geotektonika, No. 1, 43–58 (1978).
16. G. I. Govorov, V. G. Sakhno, and D. Z. Zhuravlev, "Nd–Sr Isotopy and Geodynamics of the Albian–Quaternary Magmatism in the South Kuril Islands," Dokl. Akad. Nauk **403**, 88–92 (2005) [Doklady Earth Sciences **403A**, 777–782 (2005)].

17. F. M. Gradstein, J. G. Ogg, A. G. Smith, et al., "A New Geological Time Scale," Episodes **27** (2), 83–100 (2004).
18. B.-M. Jahn, G. Gruau, R. Capdevila, et al., "Archean Crustal Evolution of the Aldan Shield, Siberia, Geochemical and Isotopic Constraints," Precambrian Res. **91**, 333–363 (1998).
19. R. W. Kay and S. M. Kay, "Delamination and Delamination Magmatism," Tectonophysics **219**, 177–189 (1993).
20. V. P. Kovach, Candidate Dissertation in Geology and Mineralogy (IGGD, St. Petersburg, 1994).
21. V. P. Kovach, A. B. Kotov, V. I. Berzkin, E. B. Sal'nikova, et al., "Age Limits of High-Grade Metamorphic Supracrustal Complexes in the Central Aldan Shield: Sm–Nd Isotopic Data," Stratigr. Geol. Korrelyatsiya **7** (1), 3–17 (1999) [Stratigr. Geol. Correlation **7**, 1–15 (1999)].
22. A. B. Kotov, I. M. Shemyakin, E. B. Sal'nikova, and V. P. Kovach, "Formation Stages and Isotope Structure of the Continental Crust of the Sutam Block, Aldan Shield: Evidence from Sm–Nd Isotope Systematics of Granitoids," Dokl. Akad. Nauk **366**, 809–812 (1999) [Doklady Earth Sciences **367**, 695–697 (1909)].
23. A. M. Larin, E. B. Sal'nikova, A. B. Kotov, et al., "The North Baikal Volcanoplutonic Belt: Age, Formation Duration, and Tectonic Setting," Dokl. Akad. Nauk **392**, 506–511 (2003) [Doklady Earth Sciences **392**, 963–967 (2003)].
24. X. Le Pichon, P. Henry, and B. Goffe, "Uplift of Tibet: From Eclogites to Granulites—Implications for the Archean Plateau and the Variscan Belt," Tectonophysics **273**, 57–76 (1997).
25. V. I. Levitskii, E. B. Sal'nikova, A. B. Kotov, et al., "Age of Formation of Apocarbonate Metasomatites of the Sharyzhalgai Uplift of the Siberian Craton Basement, Southwestern Baikal Region: U–Pb Baddeleyite and Zircon Datings," Dokl. Akad. Nauk **399**, 650–654 (2004) [Doklady Earth Sciences **399A**, 1204–1208 (2004)].
26. T. P. Litvinova, N. P. Shmiyarova, and L. V. Ermoshko, *Map of the Anomalous Magnetic Field of the USSR and Adjacent Territories, 1: 10000000* (Aerogeologiya, Leningrad, 1978) [in Russian].
27. B. G. Lutts and V. K. Oksman, *Deeply Eroded Fault Zones of the Anabar Shield* (Nauka, Moscow, 1990) [in Russian].
28. A. V. Manakov, *Structural Peculiarities of the Yakut Kimberlite Province Lithosphere* (Voronezh. Univ., Voronezh, 1999) [in Russian].
29. L. A. Neimark, A. M. Larin, A. A. Nemchin, et al., "Anorogenic Nature of Magmatism in the Northern Baikal Volcanic Belt: Evidence from Geochemical, Geochronological (U–Pb), and Isotopic (Pb, Nd) Data," Petrologiya **6**, 139–164 (1998) [Petrology **6**, 124–148 (1998)].
30. L. A. Neimark, A. A. Nemchin, O. M. Rosen, et al., "Sm–Nd Isotopic Systems in Xenoliths of Lower Crust from Kimberlites of Yakutia," Dokl. Akad. Nauk **327**, 374–378 (1992).
31. M. Nironen, B. A. Elliot, and O. T. Ramo, "1.88–1.87 Ga Post-Kinematic Intrusions of the Central Finland Granitoid Complex: A Shift from C-type to A-type Magmatism during Lithospheric Convergence," Lithos **53**, 37–58 (2000).
32. O. I. Parfenyuk, Doctoral Dissertation in Geology and Mineralogy (IFZ, Moscow, 2004)
33. O. I. Parfenyuk and J.-C. Mareschal, "Thermomechanical Model of Evolution of Layered Lithosphere in Continental Collision Zones," Ann. Geophysicae **15**, 1–19 (1997).
34. A. F. Petrov, G. S. Gusev, F. F. Tret'yakov, and V. S. Oksman, "Archean (Aldan) and Lower Proterozoic (Karelian) Megacomplexes," in *Structure and Evolution of the Yakutiya Crust*, Ed. by V.V. Koval'skii (Nauka, Moscow, 1985), pp. 9–39 [in Russian].
35. N. V. Popov and A. P. Smelov, "Metamorphic Formations of the Aldan Shield," Geol. Geofiz., No. 37, 148–161 (1996).
36. *Precambrian Geology of the USSR*, Ed. by D. V. Rundquist and F.P. Mitrofanov (Nauka, Leningrad, 1988) [in Russian].
37. C. I. Prince, J. Kosler, D. Vance, and D. Gunter, "Comparison of Laser Ablation ICP-MS and Isotope Dilution REE Analyses—Implication for Sm–Nd Garnet Geochronology," Chem. Geology **168**, 255–274 (2000).
38. V. S. Rachkov, "Deep Fault Zones," in *The Archean of the Anabar Shield and Problems of the Early Earth Evolution*, Ed. by. M. S. Markov (Nauka, Moscow, 1988), pp. 146–176 [in Russian].
39. N. G. Rizvanova, O. A. Levchenkov, I. S. Bogomolov, et al., "Comparison of Zircon Separation Methods for Geochronological Purposes," Geokhimiya, No. 7, 1076–1086 (1994).
40. H. R. Rollinson, *Using Geochemical Data: Evaluation, Presentation, Interpretation* (Longman Sci., Techn., Singapore, 1994).
41. O. M. Rosen, "Geochemistry of Granulites and the Archean Sialic Crust Formation in the Anabar Shield (Northern Siberia)," in *High Grade Metamorphics* (Theophrastus Publications, Athens, 1992), pp. 69–102.
42. O. M. Rosen, "Siberian Craton, a Fragment of a Paleoproterozoic Supercontinent," Russian Journ. Earth Sci. **4** (2), 103–119 (2002).
43. O. M. Rosen, "The Siberian Craton: Tectonic Zonation and Stages of Evolution," Geotektonika **37** (1), 1–19, (2003) [Geotectonics **31**, 175–192 (2003)].
44. O. M. Rosen and V. S. Fedorovskii, *Collision-Related Granitoids and Crustal Delamination (Examples of Cenozoic, Paleozoic, and Proterozoic Collision Systems)* (Nauchnyi Mir, Moscow, 2001) [in Russian].
45. O. M. Rosen, K. S. Condie, L. M. Natapov, and A. D. Nozhkin, "Archean and Early Proterozoic Evolution of the Siberian Craton, a Preliminary Assessment," in *Archean Crustal Evolution*, Ed. by K.S. Condie (Elsevier, Amsterdam, 1994), pp. 411–459.
46. O. M. Rosen, V. P. Serenko, Z. V. Spetsius, et al., "Yakut Kimberlite Province: Position in the Structure of the Siberian Craton and Peculiarities in the Upper and Lower Crust Composition (Data on Drill-Core Samples and Inclusions in Kimberlites)," Geol. Geofiz. **43**, 3–26 (2002).
47. O. M. Rosen, D. Z. Zhuravlev, M. K. Sukhanov, et al., "Isotopic–Geochemical and Age Heterogeneity of Early Proterozoic Terranes, Collision Zones and Related

Anorthosites in the Northeastern Siberian Craton," Geol. Geofiz. **41**, 163–179 (2000).

48. E. B. Sal'nikova, V. A. Glebovitskii, A. B. Kotov, et al., "Metamorphic Evolution of Granulites from the Kurul'ta Block, Aldan Shield: U–Pb Single Zircon Study," Dokl. Akad. Nauk **398**, 239–243 (2004) [Doklady Earth Sciences **398**, 968–972 (2004)].
49. M. P. Searle, "Extensional and Compressional Fields in the Everest–Lhotse Massif, Khumbu Himalaya, Nepal," Journ. Geol. Soc., London **156**, 227–240 (1999).
50. J. Selverstone, "Are the Alps Collapsing?," Annu. Rev. Earth Planet. Sci. **33**, 2.1–2.20 (2005).
51. M. A. Semikhatov, "Recent Precambrian General Scales: Comparison," Stratigr. Geol. Korrelyatsiya **1** (1), 6–16 (1993).
52. V. M. Shemyakin, V. A. Glebovitskii, N. G. Berezhnaya, et al., "The Age of the Oldest Rocks of the Sutam Block (Aldan Granulite-Gneiss Area)," Dokl. Akad. Nauk **360**, 526–529 (1998) [Doklady Earth Sciences **360**, 521–524 (1998)].
53. A. P. Smelov, V. I. Berzkin, A. N. Zedgenizov, et al., "New Data on Composition, Structure, and Ore-bearing Potential of the Kotuikan Tectonic Melange Zone," Otech. Geol., No. 4, 45–49 (2002).
54. A. P. Smelov, A. N. Zedgenizov, L. M. Parfenov, and V. F. Timofeev, "Precambrian Terranes of the Aldan–Stanovoi Shield," in *Metallogeny, Hydrocarbon-bearing Potential, and Geodynamics of the North Asian Craton and Bordering Orogenic Belts* (Santai, Irkutsk, 1988a), pp. 1–120 [in Russian].
55. A. P. Smelov, V. P. Kovach, V. D. Gabyshev, et al., "Tectonic Structure and Age of the Basement in the Eastern North Asian Craton," Otech. Geol., No. 6, 6–10 (1988b).
56. S. D. Sokolov, "Accretionary Tectonics: Conceptual Basis, Problems, and Prospects," in *Problems of Global Geodynamics*, Ed. by D. V. Rundquist (OGGGN RAN, Moscow, 2003), Issue 2, pp. 32–56 [in Russian].
57. V. G. Spiridonova, S. F. Karpenko, and A. V. Lyalikov, "Sm–Nd Age and Geochemistry of Granulites in the Central Anabar Shield," Geokhimiya, No. 10, 1412–1427 (1993).
58. S. R. Taylor and S. M. McLennan, *The Continental Crust: Its Composition and Evolution* (Blackwell, Oxford, 1985).
59. *The Early Precambrian of Southern Yakutia*, Ed. by N. L. Dobretsov (Nauka, Moscow, 1986) [in Russian].
60. *Map of Metamorphic and Granite Formations of the USSR, 1 : 10000000*, Ed. by B. Ya. Khoreva (VSEGEI, Leningrad, 1987) [in Russian].
61. M. Thöni, "Sm–Nd Isotope Systematics in Garnet from Different Lithologies (Eastern Alps): Age Results and Evaluation of Potential Problems for Garnet Sm–Nd Chronometry (Erratum)," Chem. Geol. **194**, 353–379 (2003).
62. O. M. Turkina, "Amphibolite–Plagiogneiss Complex of the Onot Block, Sharyzhalgai Uplift: Isotopic and Geochemical Evidence for Evolution of the Continental Crust in the Early Archean," Dokl. Akad. Nauk **399**, 678–682 (2004) [Doklady Earth Sciences **399A**, 1296–1300 (2004)].
63. A. G. Vladimirov, N. N. Kruk, S. N. Rudnev, and S. V. Khromykh, "Geodynamics and Granitoid Magmatism of Collision Orogens," Geol. Geofiz., No. 12, 1321–1338 (1978).